Universiteit
Leiden
The Netherlands

Magneto-Transport of a Reissner-Nordstrom Holographic Metal

Arend, Salomon

Citation
Arend, S. (2022). *Magneto-Transport of a Reissner-Nordstrom Holographic Metal*.

Version:	Not Applicable (or Unknown)
License:	License to inclusion and publication of a Bachelor or Master thesis in the Leiden University Student Repository
Downloaded from:	https://hdl.handle.net/1887/3285057

Note: To cite this publication please use the final published version (if applicable).

Magneto-Transport of a Reissner-Nordström Holographic Metal

THESIS

submitted in partial fulfillment of the
requirements for the degree of

MASTER OF SCIENCE
in
THEORETICAL PHYSICS

Author :	Salomon C.F. Arend
Student ID :	1096192
Supervisor :	Prof. Koenraad Schalm
	Drs. Floris Balm
Second corrector :	Prof. Jan Zaanen

Leiden, The Netherlands, January 13, 2021

Magneto-Transport of a Reissner-Nordström Holographic Metal

Salomon C.F. Arend

Lorentz Institute for Theoretical Physics
P.O. Box 9506, NL-2300 RA Leiden, The Netherlands

January 13, 2021

Abstract

The AdS/CFT correspondence provides a way to perform computations on strongly interacting, conformal systems living in the AdS boundary by studying the behaviour of the holographic dual in the form of a black hole in the centre. Until now, such inquiries where limited to spatially homogeneous systems, however, metallic systems are characterized by the presence of an ionic lattice. We study the DC magneto-transport of a dual to Reissner-Nordström metal using a novel code which numerically computes its behaviour in two dimensions in the presence of an explicit lattice and a magnetic field. We find that conductivity is dominated by Drude transport at low temperatures. Furthermore, we find that the transport is described by a transverse relaxation rate Γ_T of angular momentum in addition to a longitudinal rate Γ_L and these depend differently on temperature. This hints that AdS/CMT may provide an explanation to the anomalous temperature scaling of the Hall Angle in the strange metal phase of high T_c superconductors.

Contents

1 Introduction

1.1 Transport & Conductivity

The study of the conductivity of materials has long been limited to the transport of certain conserved quantities facilitated by the movement of (quasi)particles. For example, electric transport can be described as the movement of electrons carrying charge through a lattice, heat (energy) can be transported by electrons or phonons. A conductivity is defined as the linear response of the flow of carriers to a small applied field - which can be a temperature gradient, an electric field, a magnetic field, etc. In the case of an electric field $\vec{E}$ sourcing a current $\vec{J}$:

$$\vec{J} = \sigma \vec{E} \tag{1}$$

which is known as Ohm's law. In a real material, a certain carrier may carry different quantities, like electrons carrying electrical charge and heat through a metal, or there may be different carriers present, like phonons opening a channel for heat transport. To describe how multiple conserved quantities flow in a system which is brought out of equilibrium when an electric field and a temperature gradient are applied simultaneously, we use the generalized Fourier's & Ohm's law:

$$\begin{pmatrix} \vec{J} \\ \vec{Q} \end{pmatrix} = \begin{pmatrix} \sigma & \alpha T \\ \bar{\alpha} T & \bar{\kappa} T \end{pmatrix} \begin{pmatrix} \vec{E} \\ \frac{\vec{\nabla} T}{T} \end{pmatrix} \tag{2}$$

Here $\vec{Q}$ is the heat current, T is the temperature, and α and $\bar{\kappa}$ are the thermo-electric and thermal conductivities respectively. In this thesis we will be looking at two dimensional materials exclusively, in which case all conductivities are 2×2 matrices. In contrast to measurements on one dimensional cables which we may be used to, resistivities are the elements of the inverse matrices (not the inverse elements of the matrices), and we have $\rho_{xx} = \sigma_{xx}/(\sigma_{xx} + \sigma_{xy})$, for example.

Due to the Onsager reciprocal relations, the conductivities will be antisymmetric if time reversal symmetry is broken [47]: $\alpha = -\bar{\alpha}$ and $\sigma_{xy} = -\sigma_{yx}$, for example . In the time reversal invariant systems these matrices

are symmetric. The canonical way in which time reversal symmetry is broken is by the presence of a magnetic field. In the Results section we will be investigating magneto-transport in detail and the off-diagonal elements are anti-symmetric in all cases.

Equation (2) is a compendium of sorts for a wide variety of experimental settings available to the solid state physicist. For example, if one heats one side of a material sample, this heat will diffuse throughout the sample. If electrons (or some other charged quasiparticles, like holes) facilitate the transport of heat, charge will also invariably want to flow and produce an induced electric field: the thermal potential creates an electric potential. This is known as the Seebeck-Peltier effect and is described as the response coefficient between the applied thermal gradient and induced electric field: $\vec{E} = -\theta\vec{\nabla}T$. We can easily read off that $\theta = -\sigma^{-1}\alpha$, since we take $\vec{J} = 0$ as there is no net current actually moving through the sample [53]. Accordingly, the Seebeck coefficient can be a measure of the particle-hole asymmetry in a given material, for example.

The goal of the theoretical effort has been to find expressions for the thermo-electric conductivities in terms of the properties of a material and its thermodynamical quantities.

1.2 Drude Theory

The first quantitative theory of the conductivity of metals was written down in 1900 by Paul Drude [17]. It is a purely classical model which assumes Newtonian point-like objects, the electrons, which are only affected by an electric field via the Lorentz force and by the ionic lattice, which they bump into and subsequently lose momentum to. The latter part, which may be a difficult affair, is modeled by introducing a relaxation rate τ (the frequency of bumps, or mean free time) which leads to momentum leaking out of our system. This gives the equation of motion:

$$\frac{d}{dt}\langle \boldsymbol{p} \rangle = q\left(\boldsymbol{E} + \frac{\langle \boldsymbol{p} \rangle \times \boldsymbol{B}}{m} - \frac{\langle \boldsymbol{p} \rangle}{\tau}\right) \tag{3}$$

where q is the electrical charge of a carrier and $\langle \boldsymbol{p} \rangle$ is the averaged momentum. Noticing that the current is related to momentum via $\vec{J} = \frac{nq}{m}\vec{P}$, since we obtain velocity by dividing out the carrier mass m and must then multiply by carrier charge and carrier density n to obtain units of current, we can rewrite above expression into the form of equation (1), and in doing so we obtain the historically first theoretical underpinning of Ohm's

law. In one dimension and taking $B = 0$ we have:

$$\sigma_{Drude} = \frac{nq^2}{m} \frac{1}{\frac{1}{\tau} + i\omega} \tag{4}$$

Here we got rid of the time derivatives by applying the identity $\boldsymbol{p}(t) = \int \hat{\boldsymbol{p}}(\omega) e^{i\omega t} d\omega$ which gives us a factor of $i\omega$, and the conductivity as a function of the frequency of the applied AC electric field: the (complex) optical conductivity. In the remainder of this thesis, we will take $\omega = 0$, and exclusively look at the DC conductivity, as these values can be efficiently computed in a holographic setting, whereas the optical conductivity in more than one dimension and in presence of a magnetic field requires a more complex numerical approach and falls outside of the scope of this work. We end up with:

$$\sigma_{DC} = \omega_p^2 \tau. \tag{5}$$

where we have defined the plasmon frequency as $\omega_p = q\sqrt{n/m}$. In the Drude model, in one dimension with no magnetic field present, the conductivity is directly proportional to the relaxation rate, multiplied by a factor which is called the Drude weight, which is the plasmon frequency squared. Plasmons are the particles related to translational symmetry breaking of our conducting medium: plasmons are to a plasma (a fluid of charged particles, as electrons in a solid) what phonons are to the ionic lattice.

From this same picture we can also derive an expression for the thermal conductivity κ, which is simply that for a kinetic gas: $\kappa = \frac{1}{3}\bar{v} n m c_V l$ where c_V is the heat capacity and l is the mean free path. We observe what happens when we inspect the ratio of thermal and electrical conductivity:

$$\frac{\kappa}{\sigma} = \frac{\bar{v} m^2 c_v l}{3q^2\tau} = \frac{8k_B^2 T}{\pi q^2} \equiv LT \tag{6}$$

since $c_V = 3\frac{k_B}{m}$ for a kinetic gas and $l = \tau\bar{v}$ and we have defined the temperature independent Lorentz factor L. This result of Drude theory is the Wiedemann-Franz law which states that the ratio of thermal and electrical conductivity is proportional to temperature, found to be true for most conventional metals across a range of temperatures [21].

1.3 Fermi Gas & Electron Band Theory

Drude theory fails to explain the existence of insulators and semi-conductors, which show increasing conductivity as a function of temperature. In the

Drude picture, $\sigma \sim \tau$, and with increasing temperature the ionic lattice shakes more violently, enlarging the cross section of scattering events, decreasing τ, showing behaviour as seen in conductors. It turns out the Pauli exclusion principle is failed to be taken into account, which states that multiple fermions cannot inhabit the same quantum state.

A Fermi gas is nothing else than a multiple particle version of the particle in an infinite square potential well, a classic exercise of Quantum Mechanics. One solves the Schrödinger equation with boundary conditions $\Psi(x) = 0$ for $x < a/2$ and $x > a/2$ for a well with size a. One gets energies $E_n = \frac{n^2\pi^2\hbar^2}{2ma}$ where n enumerates the exited states and the ground state is $n = 1$. The Fermi gas takes these solutions and fills the energy levels from the ground state up until we run out of particles. Since there are no interactions the levels are not affected, and we take V to be the size of our solid: $V = l^3$. In a classical gas, the chance to find a particle with energy ϵ is given by the Maxwell-Boltzmann distribution:

$$n_{\mathrm{MB}}(\epsilon) = e^{-(\epsilon-\mu)/k_B T} \tag{7}$$

In a Fermi gas, due to the anti-symmetrization of the wave function with respect to to identical fermions, this is replaced by the Fermi-Dirac distribution:

$$n_{\mathrm{FD}}(\epsilon) = \frac{1}{e^{(\epsilon-\mu)/k_B T} + 1} \tag{8}$$

The effect of temperature is to blur the hard border of our Fermi sphere: in the $T \to 0$ case, we obtain a Heaviside function with a discontinuity at $\epsilon_F = \mu$, which we call the Fermi energy. The Fermi energy is the energy at the Fermi surface, the border between filled and unfilled states in phase space.

Already our Fermi gas is quite different to the ideal kinetic gas which was used in the Drude model, as it is characterized by a Fermi surface and exhibits *degeneracy pressure*, which actually accounts for the solidity of most common materials, built up from fermions [18]. However, we need one more ingredient in our system to link it to conductivity as seen in experimental settings, and that is, of course, the ionic lattice in which our electrons live. It turns out that simply requiring that the potential to be periodic, and not worrying about the intricate details of how atomic nuclei would interact with electrons, is enough to reach our goal. This result is known as Bloch's theorem. Following [22], we have:

$$V(x + a) = V(x) \tag{9}$$

and for ease of use we make it periodic with N periods so that $V(Na) = V(0)$. If we define a displacement operator $Df(x) = f(x + a)$, we notice

that it commutes with our Hamiltonian which is also periodic. This means they can be simultaneously diagonalized:

$$\psi(x+a) = \lambda\psi(x) \tag{10}$$

with ψ an energy eigenstate and λ some complex number. Also note that:

$$\psi(x+Na) = \psi(x) \implies \lambda^N\psi(x) = \psi(x) \implies \lambda^N = 1. \tag{11}$$

Now let us look at the Schrödinger equation within the periodic lattice, and assume the potential has no bearing within these regions, and so is in some way spiked: electrons only notice the nuclei from very short distances as compared to the interatomic spacing a - and when close to the nuclei, the potential becomes effectively infinite. In that case, we are dealing with a periodic infinite square well with Hamiltonian:

$$-\frac{\hbar^2}{2m}\frac{d^2\psi}{dx^2} = E\psi, \tag{12}$$

and solution:

$$\psi(x) = A\sin(kx) + B\cos(kx) \tag{13}$$

within these free regions, where $k \equiv \frac{\sqrt{2mE}}{\hbar}$. Writing $\lambda = e^{iKa}$ (which implies $K = \frac{2\pi n}{Na}$) since $|\lambda|^2 = 1$ must hold, and applying this to equation (13) to jump to the cell immediately left of the origin we get:

$$\psi(x) = e^{-iKa}[A\sin k(x+a) + B\cos k(x+a)] \tag{14}$$

Equation (13) and (14) must be equal at $x = 0$. which gives us:

$$B = e^{-iKa}[A\sin(ka) + B\cos(ka)]. \tag{15}$$

Multiplying by e^{iKa}/B and taking only the real part we get:

$$\cos(Ka) = \frac{A}{B}\sin(ka) + \cos(ka). \tag{16}$$

We can see that, generically, there are not always solutions for any given energy $E \sim k^2$ since we can choose $|\frac{A}{B}| > 1$ and the left hand side can never exceed 1. Furthermore, there will also always be regions for values of k where solutions do exist: these are called *bands* and they are separated by *gaps* of forbidden energies.

These bands are filled up from the bottom up, following the Fermi-Dirac distribution. The crucial question now is, of course, where is the

Fermi energy as compared to our bands? Depending on the amount of valence electrons in the outer shell of the atoms in our material, and any doping which of course adds holes or extra electrons into the mix, the outer most band may be either filled or partially full. In the case of a partially filled outer band, which means the Fermi energy lies somewhere in the middle of a band, relatively small energies suffice to excite electrons into conductive channels within the material, since they lie within a band - this is called a conductor. If the band is filled, any excitations will also need to bridge the gap which requires a much larger energy for the electrons to end up in the next band - this means the material is an insulator. Doping the material may produce a semi-conductor accordingly. Furthermore, if one increases temperature, this means more electrons will end up in the conducting band in the case of an insulator, making the jump with the help of thermal fluctuations: insulators will conduct better with higher temperature - this immediately follows looking at the Fermi-Dirac distribution. This concludes how the Fermi gas model of an electron system predicts the existence of insulators and semi-conductors as found in nature.

1.4 Fermi Liquid Theory

Departing from a Fermi gas, we may wonder what happens when we introduce electron-electron interactions. As we know, they do indeed exist in the form of the Coulomb potential, and we may hope including them more accurately describes electrons in a solid than the Fermi-gas band-gap theory. Landau wrote down the phenomenological theory in an effort to describe Helium-3, which are fermions with slight interactions, in what has now become known as Fermi liquid theory [36]. It is an effective description of fermions at low temperatures compared to the Fermi level ($k_B T \ll \epsilon_F$) with significant interactions.

Landau's argument boils down to that there is a one-to-one correspondence between the excitations of the interacting theory and the particles of the non-interacting theory: the Fermi gas. This means that we can effectively describe a Fermi liquid as a Fermi gas of quasiparticles (the excitations around the Fermi-surface): the properties of the quasiparticles take all the effects of interactions into account - we use the quasiparticle mass and charge in defining the plasmon frequency $\omega_p = nq_*^2/m_*^2$ in equation (5). In the zero temperature case, a single electron lying above the Fermi surface with energy ϵ_1 can scatter with one lying in the Fermi sea with energy ϵ_2 into two states lying above the Fermi surface with energies ϵ_3

and ϵ_4. We have $\epsilon_1 + \epsilon_2 = \epsilon_3 + \epsilon_4$. Given our first electron, we have a sliver above the sphere with of length $|\epsilon_1 - \epsilon_F|$ to scatter into - the size of this sphere determines our scattering probability (the amount of states permissible taking conservation of energy into account). Since, given ϵ_1, we have two choices in energy levels (e.g. ϵ_4 is determined once we have chosen the other two) the scattering rate goes as $|\epsilon_1 - \epsilon_F|^2$. In the finite temperature case, the Fermi surface is blurred with a width $k_B T$, and thus we pick up a contribution to our scattering rate $\frac{1}{\tau} \sim (k_B T)^2$ - as now the available phase space is determined by the temperature more so than the energy of the first exited electron. We, therefore, find the DC resistivity of the Fermi liquid to be quadratic in temperature:

$$\rho_{DC,FL} = \frac{1}{\sigma_{DC,FL}} \sim T^2. \tag{17}$$

Another characteristic of the Fermi liquid is its entropy. The entropy is, of course, the uncertainty with regard to the exact state the system is in. Taking again the image of the Fermi surface being blurred by increasing temperature, we can easily guess what it is: $S \sim T^{d-1}$. The fact that all excitations lie around a surface effectively removes one dimension from phase space: this is the Sommerfeld entropy.

One of the central assumptions of Fermi liquid is the stability of the quasiparticles, expressed as $\tau \gg \hbar / k_B T$ (where τ is the particle lifetime) and we shall later see it is exactly this assumption which seems to be violated in strange metals. This means the quasiparticle picture in general does not hold and a widely different approach is needed. Note that this has nothing to do with the 'wave/particle' duality: given a many-particle wavefunction we can often find a Hermitian operator, for which the corresponding basis neatly orders the wavefunction into a product state of its tensor elements. In the case of the momentum operator, we can call these states 'waves' and in the case of position we call these 'particles', however, more generally, the fact that the wavefunction decomposes into a product makes that we call these states (quasi)particles for any arbitrary corresponding operator. Thus, our particles may be purely wavelike. For very complex states which cannot be written as product states, and highly entangled states are examples of this, we say there are no quasiparticles. However, no rigorous method exists to conclude no operator of the kind exists for a given wavefunction.

NOTE: While electron-electron interactions as described above conserve energy, they, in fact, do not typically conserve momentum when the Fermi liquid is embedded in a lattice. Due to the Umklapp process, when the initial wave vectors are sufficiently large, the resulting particles can

have a flipped momentum: momentum has dissipated out of the electron system into the lattice. That is the reason why the quasiparticle lifetime τ, associated with their rate of interaction, is also a measure for momentum dissipation of the Fermi liquid, and sets the resistivity. Due to the particles living on the Fermi surface, their energies are quite small (seen from the Fermi surface) as compared to their momenta (seen from the origin) - this makes Umklapp scattering possible even at low temperatures.

NOTE: As described above, resistivity will go like T^2 in Fermi liquids like metals at low temperatures, however, when one measures the temperature dependence resistivity, one will most likely find different a scaling. This is because we only took electron-electron interactions into account. If we increase temperature, a lot more phonons will start to populate our material, as higher frequency modes will become available to them until we reach the Debye frequency - phonon densities will increase with T^3 and because of how their interactions are angle dependent with $\cos\theta$ we pick up another T^2 term giving us $\rho \sim T^5$ for electron-phonon interactions. At even higher temperatures, where we have passed the Debye temperature, and all of phase space is equally accessible for our phonons, they will start to behave like classical springs and we can deduce from the equipartition theory that they now increase linearly in T, as is measured for resistivity in metals at high temperatures.

1.5 Superconductivity & BCS Theory

In 1911 it was discovered by Heike Kamerlingh Onnes in Leiden that mercury loses its resistivity altogether when cooled below 4.2K [33]. Materials which possess such superconducting properties have drawn attention because of their many useful applications, mostly based on generating very large magnetic fields by induction, using currents which would otherwise melt the components if even a little resistance remained and was allowed to generate heat. Examples of technologies currently utilizing superconductivity are MRI's, nuclear fusion reactors, using the magnetic fields to contain the fusing plasma [19] and particle accelerators such as the LHC [48].

On the other side, superconductivity drew the attention from the theoretical community as how to account for this phenomenon of vanishing resistivity - which one would naively not expect to happen at any finite temperature (for a Fermi liquid with $\rho \sim T^2$, resistivity only vanishes at zero temperature). The solution was found by Bardeem, Cooper and Schrieffer in what is now known as BCS theory [7]. It departs from a Fermi

Version of January 13, 2021– Created January 21, 2022 - 14:18

liquid with a slight *attractive* interaction V_0 between the fermions. In metals, phonons mediate this interaction between electrons. The isotope effect was the hint that the lattice plays a role in the phenomenon: it was found that $T_C \sim M^{-1/2}$ where M is the atomic mass of the material [16].

The next experimental hint was the fact that the specific heat exponentially decays at the critical temperature T_c, indicating that there was a large reduction in the density of states at this point (so that a little extra energy immediately fills all available states), which meant there has to be a gap in the energy spectrum at T_c. A normal Fermi liquid metal is characterized by gapless excitations around the Fermi surface as discussed in the previous section, which is why electrons are easy to excite into conducting states.

The crucial ingredient to BCS theory is precisely the existence of a well defined Fermi surface, which is why we have to depart from a Fermi liquid: this makes it so that the attractive interactions between the particles can only happen in small halo around the surface, and only the density of states at this point in phase space is relevant. After some calculations, this fact turns out to lead to a negative binding energy for pairs of fermions *for any* V_0, no matter how weak. Another way of putting it, is that a gap springs into existence at low temperatures which protects these pairs from decaying - which is why they can travel unhindered through the material with zero resistivity. The gap at zero momentum is given by:

$$\Delta_0 = 2\hbar\omega_D e^{-\frac{1}{V_0\rho_F}} \tag{18}$$

where ω_D is the Debye frequency (the maximum frequency of phonons in a lattice, set by the lattice spacing and atomic weight) and ρ_F is the density of states at the Fermi surface. The critical temperature is given by:

$$T_c = \frac{e^{\gamma_E}}{\pi k_B}\Delta_0 \tag{19}$$

where $\gamma_E \approx 0.577$ is the Euler constant. We see that no matter how small we choose V_0 to be, T_c will always be some finite value. Another satisfactory result is that T_c is proportional to ω_D, which goes as $M^{-1/2}$, explaining the isotope effect.

The bound pairs, called Cooper pairs, are made up of a duo of fermions and are thus bosons themselves: this makes them able to all condense into the ground state at sufficiently low temperatures, forming a Bose-Einstein condensate - even though the electrons they are made up of are all still neatly occupying some unique state in phase space. This entire story does not only explain superconductivity in metals, but also superfluidity

in fermionic Helium-3 via the exact same mechanism. Here there is, of course, no lattice for phonons to mediate an attractive interaction - and it is the Van der Waals force that makes ^{3}He stick together into pairs [56]: as predicted by BCS theory, the specific nature or even magnitude of the force is not of the essence, as long as it is attractive there is some condensation temperature.

NOTE: Another way to look at superconductivity is with a mean field method, where one can see that the gap Δ is actually the order parameter of the condensate phase, breaking local $U(1)$ gauge symmetry [1]. As this is not a global symmetry, we do not end up with a Goldstone boson, but instead, 'the photon acquires mass' via the Anderson-Higgs mechanism. The same idea was later applied to particle physics to explain the mass of elementary particles. In a superconductor, the mass of the photon means electric and magnetic fields are mediated by a massive particle, which makes its effects very short ranged ($\sim e^{-m_{Ph}r}$ instead of $\sim 1/r$) and thus we have phenomena like magnetic fields being expelled from the insides of superconductors in what is known as the Meissner effect.

From equation (19) one can deduce some upper bound for the maximal attainable critical temperature to be found in nature, which is known as McMillan's limit, and lies somewhere around 40K [41]. In 1986, a major experimental discovery was made in the form of the first high temperature superconductor, breaking the limits of which had been possible in BCS theory [9]. Nowadays, these copper-oxide compounds (cuprates) have been known to have a critical temperatures as high as 133K [52]. Moreover, it are precisely these materials which defy Fermi liquid theory at temperatures above their critical temperature... It is clear some new framework of conductivity and transport is needed in dealing with these challenges brought forth by experiment.

1.6 High-Temperature Superconductivity

Let us first go over the experimental findings in the field of high temperature superconductors. The most salient feature is the high T_c, with the record being 133K as mentioned, higher than permissible by BCS theory. However, when trying to discern what goes on within these materials, superconductivity may actually be an antagonist, as we have no probe for resistivity as function of temperature, and the Meissner effect dispelling magnetic fields makes the study of magneto-transport impossible. Thus, we investigate these materials above their critical temperature. Here, a plethora of strange transport behaviour is to be found. First and foremost,

Version of January 13, 2021– Created January 21, 2022 - 14:18

these materials exhibit a linear in T resistivity going up directly from the origin at zero T all the way up to the melting point of the material [31]. (One can effectively turn off superconductivity by turning on a very strong magnetic field, to measure finite resistivity at low temperatures.) This is in direct contradiction with Fermi liquid predictions as discussed in section 1.4, where we expect different regimes of T^2 and T^5 behaviour before it saturates for linear in T only at high temperatures. That cuprates seem to ignore these subtleties is quite puzzling.

Another surprising feature is that the Hall angle, which is the ratio of transverse and longitudinal conductivity σ_{xy}/σ_{xx}, has a $1/T^2$ temperature dependence, *different from the linear in T longitudinal resistivity* [46]. Regarding this finding, which has not been explained using conventional Fermi liquid theory and central to the magnetotransport of cuprates, we will go into more detail later, and show that Holographic metal theory predicts different temperature scaling of the Hall angle and longitudinal resistivity in section 3.6.

In most metals, one can lower the longitudinal resistivity by applying a magnetic field perpendicular to the plane of flow: the electrons start performing cyclotron motion and are deflected, raising resistance. This phenomenon is called magnetoresistance (MR). While the MR in common metals adheres to Kohler's law, cuprates surprise us once again and show what is called 'Planckian quadrature' in the overdoped regime, and a modified version of Kohler's law in the underdoped regime [2]. We study the MR of our RN metal in section 3.9.

There are more strange characteristics of these materials to be listed, however, those mentioned above are the most relevant to our current research and observations listed in the results section.

What exactly are these high temperature superconducting materials made out of? There are a number of different classes, but here we will focus on the cuprate based substances. Essentially, they are structured from two dimensional layers of copperoxide, with layers of other materials between them, such as Lanthanum-Barium (LB-CuO), Yttrium-Barium (YB-CuO) and Bismuth-Strontium-Calcium (BiSC-CuO)[34]. These layers do not participate in transport and act as a charge reservoir for the conducting copper oxide layers between them, effectively doping the system. By doping we add or remove electrons from our system, which is a crucial parameter in exploring the behaviour of cuprates, as we enter widely different regimes and phases when altering the doping and temperature, shown in the famously complex phase diagram (simplified here) in figure 1.

Going from optimal doping, where we find our highest T_c and strange

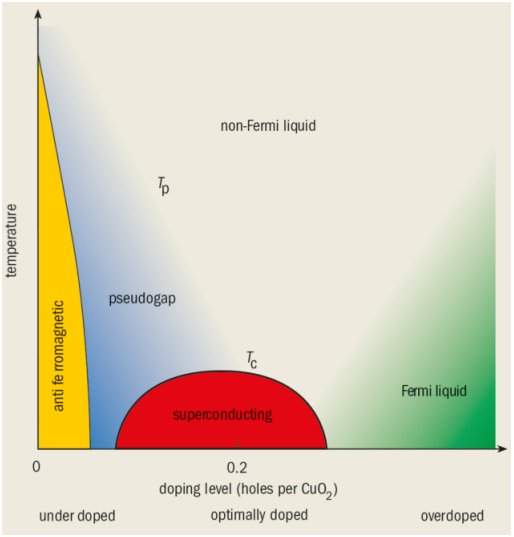

Figure 1: *Phase diagram of cuprate as a function of temperature and doping as from [8]. As we move from underdoped to overdoped, we go from an anti-ferromagnetic Mott insulator via the pseudogap and Non-Fermi liquid Strange metal phase to the normal metallic phase at high doping. The superconducting dome lies mostly under the Strange metal phase, with its peak at optimal doping.*

metal behaviour and increasing doping drastically, removing electrons as we go, we find we reenter the domain of normal metallic behaviour as described by Fermi liquids with a well defined Fermi surface [55]. It is always good to have a charted area as a starting point - what exactly could be going wrong as we increase the electrons density? An easy guess it that it would have to be something to do with electron-electrons interactions, as those are reduced with the electron density... Let us check in the highly underdoped regime: here we find our cuprate to be an anti-ferromagnetic insulator known as a Mott insulator, a system characterized by its enormous electron-electron interactions. It seems we were on the right path with our guess. Let us take a closer look at these materials.

1.7 Mott Insulators

Cuprates descend from a parent Mott insulator by doping them to some critical value. What are Mott insulators? In a certain sense Mott insulators are the exact opposite of a Fermi liquid/gas system: where these are characterized by free moving electrons in momentum eigenstates with negligible interactions, the electrons in a Mott insulator are in position eigenstates, dominated by their strong interactions and have negligible kinetic

energy. They are the ordered, potential dominated version of the Fermi gas and can perhaps be understood as a Fermi crystal. Why they are insulators is not hard to see: the electrons are locked in a kind of traffic jam, where, if one electrons where to hop to the next atom, all electrons in the material would have to hop at the same moment [34]. Note that the mechanism for their insulating behaviour is completely different from that of the band-gap theory, which actually predicts most Mott insulators to be good conductors [44]. It appears the chemistry of the cuprates amplifies the Coulomb interactions between electrons in the outer shells to a large degree.

Mott insulators can be effectively described by the Hubbard model, which is deceivingly simple, here given for one dimension:

$$\hat{H}_{Hubbard} = -t\sum_{i,\sigma}(\hat{c}^{\dagger}_{i,\sigma}\hat{c}_{i+1,\sigma} + \hat{c}^{\dagger}_{i+1,\sigma}\hat{c}_{i,\sigma}) + U\sum_{i}(\hat{n}_{i\uparrow}\hat{n}_{i\downarrow}). \tag{20}$$

It describes spins $\hat{c}_{i,\sigma}$ sitting at lattice sites i with hopping potential t and repulsive interaction U. $\hat{n}_{i,\sigma} = \hat{c}^{\dagger}_{i,\sigma}\hat{c}_{i,\sigma}$ is of course the spin density operator. Depending on the ratio U/t this describes a a perfect insulator in the $U/t \to \infty$ limit, where it becomes identical to a tight binding system, or an (anti)ferromagnetic system of spins if U/t is not too large [30]. In fact, analytical solutions to the Hubbard model in arbitrary dimensions have not been found. Why is this the case? Most likely, it has to do with the fact that these systems are strongly interacting, or, strongly correlated.

Perturbation theory is based on the principle that one can get predictions to arbitrary accuracy by performing an expansion around the solution to the non-interacting case in powers of the interaction coefficient g (coupling constant). It can easily be seen that this ploy only works when $g < 1$ in whatever units we have chosen, as higher terms will be increasingly irrelevant to the final outcome. A famous example is Quantum Electrodynamics (QED) where the coupling constant is the Fine Structure constant $\alpha \approx \frac{1}{137}$ and Feynman diagrams provide a way to keep track of the expressions of higher order terms. The opposite is true in strongly interacting systems which are defined as having $g > 1$: the higher the term the more relevant it is, and there is no hope of using perturbation theory in these cases. Quantum Chromodynamics (QCD), describing the strong nuclear interactions as the exchange of virtual gluons via a $SU(3)$ gauge symmetry, is the famous counterpart to QED. Except in the case of very high energies where asymptotic freedom kicks in, one needs other methods than perturbation theory to make predictions within QCD.

That strange metal cuprates descend from a parent Mott insulator is a strong indication that they in fact are strongly coupled systems. Fur-

Version of January 13, 2021– Created January 21, 2022 - 14:18

thermore, another hint that strong correlation is causing the strange metal behaviour, is given by the experimental fact that the linear in T resistivity is observed in multiple systems where electrons are know to be strongly correlated, even though they may not exhibit high T_c superconductivity [31].

1.8 Strongly Interacting Systems

As described above, strongly interacting systems present a challenge to analytical methods, however, cases exist where theory did indeed gain a foothold in these domains. One method is to unleash the power of modern supercomputing clusters on the equations of motions and simply brute force a way into a solution, as is done in Lattice QCD - which can, of course, always be done in principle, but is highly resource intensive. Are there more elegant approaches?

Take the action describing photon propagation in quantum field theoretic (QFT) language:

$$S[\mathbf{A}] = -\int dx^4 \frac{1}{4g^2} F_{\mu\nu}^2. \tag{21}$$

When we include charged fermions (such as electrons described by a spinor field) interacting with our vector potential we get the complete theory of electromagnetism (QED). Here $F_{\mu\nu} = \partial_\mu A_\nu - \partial_\nu A_\mu$. Taking $\delta S = 0$ we find the EoM:

$$\partial_\mu F^{\mu\nu} = J^\nu_{\text{Electric}}, \tag{22}$$

in the general case with charged particles (for our vacuum case equation (22) is 0). Note that equation (22) together with Bianchi's identity, $\partial_{[\mu} F_{\nu\rho]} = 0$, gives us all four of Maxwell's equations. (The square brackets around the indices denote that the tensors are anti-symmetrized in these indices.) Let us now take Bianchi's identity as the EoM and supply it with a four current:

$$\partial_{[\mu} F_{\nu\rho]} = \epsilon_{\mu\nu\rho\sigma} J^\sigma_{\text{Magnetic}}. \tag{23}$$

Note that, in Maxwell equation notation, now $\nabla \cdot \mathbf{B} \neq 0$: we have acquired a magnetic charge in the process, also known as the magnetic monopole. We can build the Bianchi identity into the action with a Lagrange multiplier $\tilde{A}$:

$$S[\mathbf{A}, \tilde{\mathbf{A}}] = -\int dx^4 \left(\frac{1}{4g^2} F_{\mu\nu}^2 + \tilde{A}^\mu \epsilon_{\mu\nu\rho\sigma} \partial^\nu F^{\rho\sigma}\right). \tag{24}$$

Version of January 13, 2021– Created January 21, 2022 - 14:18

By completing the squares on $F^{\mu\nu}$ we can integrate it out completely and are left with:

$$S[\tilde{\mathbf{A}}] = -\int dx^4 \frac{g^2}{4}(\partial_{[\rho}\tilde{A}_{\sigma]})^2 = -\int dx^4 \frac{g^2}{4}\tilde{F}^2_{\rho\sigma}. \tag{25}$$

We see that this is identical to the original action (21), with the transformation $g \to 1/\tilde{g}$. Therefore, there exists a dual description of electromagnetism in terms of magnetic monopoles instead of electric charges, known as the Montonen-Olive duality [43]. The crucial element here is that it is a *strong/weak* duality: trying to perturbation theory in the magnetic case has no hope of succeeding, however, transforming to the electric dual description inverts our coupling constant g and we enter a weakly interacting theory. Thus, if one is able to find a strong/weak duality for a strongly interacting theory, the validity of perturbation theory is restored. Is there such a duality available for our strongly interacting, doped Mott insulator cuprate system?

1.9 AdS/CFT Correspondence

We must first note that it is believed there is a phase transition taking place in the cuprates at critical doping [50]. As is known from Renormalization Group theory, critical points signal the onset of scale invariance in a system as driven by temperature. However, here it is driven by doping - as we have seen in figure 1, doping is a way to effectively tune the coupling coefficient of our system from dominant (Mott phase) to negligible (Fermi liquid phase). Imagine a Hamiltonian with a potential term proportional to g - if we slowly vary g, the energies of all the Hamiltonian eigenstates will also continuously shift accordingly. It may happen that the energy of some eigenstate may suddenly acquire an energy lower than the groundstate and become the new groundstate at a critical coupling g_c: therefore, we get a sudden jump in the structure of our groundstate (even though all states vary smoothly as a function of g). This is called a Quantum Phase transition at a Quantum Critical Point (QCP) [51]. Such a transition can take place at zero temperature, furthermore, it is found that even at non-critical coupling, quantum critical behaviour is restored at finite temperature, resulting in the famous quantum critical wedge. A system in a quantum phase transition may be described by a conformal field theory (CFT) which is a Quantum Field theory endowed with conformal invariance. Barring many subtleties and the unsolved question concerning the presence of a QCP in cuprates, let us for now suppose a cuprate at critical doping can be effectively described by a CFT.

It was noticed by Maldacena that there is a special relationship between CFTs in d-dimensions and AdS space in d+1 dimensions [39]. Anti-de-Sitter space is a maximally symmetric, vacuum solution to the Einstein equation, which describes gravity in terms of the curvature of space-time with the metric tensor $g_{\mu\nu}$ as the dynamic field. In Euclidean geometry, the maximally symmetric spaces are the sphere, flat space and hyperbolic space: Anti-de-Sitter space is the Lorentzian equivalent of hyperbolic space, characterized by a negative cosmological constant, or a negative inherent curvature. The metric tensor in AdS is given by:

$$ds^2 = \frac{1}{y^2}\left(-dt^2 + dy^2 + \sum_i dx_i^2\right) \tag{26}$$

Here, y is the radial coordinate where $y \to \infty$ is the centre of our space. It is easily seen that as we transform all spatial coordinates $(y, x_i) \to (\lambda y, \lambda x_i)$, our metric remains unchanged: it is scale invariant. Furthermore, AdS possesses the curious feature that it reduces to a flat Minkowski space at infinite spatial distance from the centre, as we take $y \to 0$ we get: $ds^2 = -dt^2 + \sum_i dx_i^2$. This infinitely far away region thus has a well defined structure, and is called the boundary of AdS. The finding of Maldacena was that, in the context of string theory, if one defines a CFT living on the conformal, Minkowski boundary of AdS, this theory is dual to the gravitational theory in the bulk. The crucial discovery was that this also was an instance of a strong/weak duality...

This is very promising, as it would allow us to actually perform calculations on our strongly interacting CFT which is quite impenetrable to ordinary analytical methods, by performing the calculations in the weakly interacting bulk dual of our AdS space and then translating back. A dictionary has been composed for this very purpose linking expectation values on the boundary to those in the bulk, knows as the Gubser-Klebanov-Polyakov-Witten (GKPW) rule:

$$\langle e^{\int d^d x J(x) O(x)} \rangle_{\text{CFT}} = \int D\phi e^{-S_{\text{AdS}}}|_{\phi(x,\partial\text{AdS})=J(x)} \tag{27}$$

for some field ϕ sourced by J and an operator O. One can churn the mathematical gears, and find that, for example, the stress energy tensor in the boundary (so what would describe the energy, pressure and shear terms of our conformal metal) $T^{\mu\nu}$ is given by the metric tensor $g^{\mu\nu}$ in the bulk. The source of our operator O in the boundary CFT is given by the leading part of the value of the field ϕ on approaching the boundary -the vacuum

Version of January 13, 2021– Created January 21, 2022 - 14:18

expectation value (VEV) of O is given by the subleading part of ϕ on approaching the boundary.

This tells us how to relate operators in the boundary to fields in the bulk, but imagine we want to implement thermodynamical aspects in the gravitational bulk theory, how would we go about that? Certainly, the cuprate systems exist at a certain temperature, posses a chemical potential, a charge density, an entropy and so forth. To understand the relationship between thermodynamics and gravity, we have to turn to Hawking's famous finding that black holes radiate light via black body radiation at a temperature given by [29]:

$$T_{\mathrm{BH}} = \frac{\hbar c^3}{8\pi G k_B M} \tag{28}$$

where M is the black hole mass and G is Newton's constant. Temperature is the exchange rate between entropy and energy, so a black hole having a temperature implies it has some entropy. This is given by the Bekenstein-Hawking formula:

$$S_{\mathrm{BH}} = \frac{c^3 k_b A}{4G\hbar} \tag{29}$$

where A is the *area* of the black hole (proportional to the Schwarzschild radius squared).

Furthermore, it was Bekenstein who recognized that black holes having an entropy sets an entropy limit on *all* forms of matter, in what is known as the Bekenstein bound. Imagine having an object of mass m, with entropy S and general length scale R and throwing this object into a black hole. The entropy of an object can be seen as the amount of bits needed to describe its exact state, or the amount of bits we are missing in knowing its full description, which can also be seen as the amount of 'chaos' in system - although this last expression can be misleading, as an ordered material like a crystal also has a finite entropy. Now, the mass of the black hole increases with that of the object, and so does the Schwarzschild radius as $r_S = 2GM/c^2$. As the radius increases, so does the area, and thus we know how much the BH entropy increases: δS_{BH}. However, imagine we chose $S > \delta S_{BH}$: it would mean information has been destroyed, or, that the entropy of our total initial system $S + S_{BH}$ would be higher than that of our final state $S_{BH} + \delta S_{BH}$, in contradiction with the second law of thermodynamics. This is not permissible, and sets an upper bound on the entropy of our object given by: $S < 2\pi R m c^2$ [10]. This is a generic trait of all matter in a theory which includes both quantum mechanics and gravity.

Version of January 13, 2021– Created January 21, 2022 - 14:18

A crucial feature of equation (29) is that the entropy/information content of a black holes goes as the *surface* the black hole, not as the *volume*, as one might naively expect. Combined with the Bekenstein bound, this has profound implications for the maximum information content of all matter and things: it scales with their area. Therefore, the information needed to describe the state of all quantum fields in a room goes as the area of the walls surrounding it, not as the volume of the room. This has become known as the Holographic principle, and was first recognized by 't Hooft in 1993 [54]. AdS/CFT is, in essence, the first mathematically applicable and precise realization of the Holographic principle: a d-dimensional Anti-de-Sitter space contains the same amount of information as the d-1 dimensional CFT on the boundary.

Thus, the thermodynamics in the boundary theory is described by black hole thermodynamics living in the centre of our AdS space. As we require our CFT to possess a charge density (it should be made up out of electrons, after all), we need our black hole to charged. This is not a generic feature of a Schwarzschild black hole, but is described by the Reissner-Nordström solution to the Einstein equations [14]. On top of that, to study magneto-transport, our CFT needs to be exposed to a magnetic field, leading us to a black hole which has both electric and magnetic charge, and we end up with an dyonic AdS Reissner-Nordström black hole [13].

Furthermore, the BH entropy is conjectured to be equal to the entanglement entropy of the boundary CFT [49]. Therefore, these conformal, quantum critical systems in the boundary may be incarnations of what one could call maximally entangled quantum matter, or densely entangled matter - as the entanglement entropy satisfies the Bekenstein bound and cannot be any higher (black holes, of course, exactly satisfy the Bekenstein bound). The highly dense many-body entanglements may mean these kinds of materials can only be microscopically simulated with the help of a Quantum computer as classical computers cannot handle the exponential complexity of the Hilbert space needed to describe them, and can hence be termed 'Quantum Supreme Matter' [58]. Holography, however, may provide a shortcut in obtaining theoretical predictions on the transport behaviours of these types of quantum matter *pur sang*.

In our case of transport of strange metals, we do not have a CFT in a spatial in a spatial continuum, so we must introduce some periodic lattice, responsible for Umklapp and band structure in ordinary materials. A lattice imposed on the boundary is dual to hair growing on the horizon (a counterexample to the no-hair theorem). This is done by modulating the chemical potential on the boundary explicitly, in our case with a square lattice [5]. A major problem arises, though: our clever ploy

of making things computationally tractable with the strong/weak duality collapses, because the lattice activates all the highly complicated nonlinearities present in the Einstein equation in the bulk. Therefore, numerical methods are required to say anything about transport properties of Holographic metals. These are explained in more detail in the Methods section.

There is one further twist to the story: the radial direction of AdS space, what is called the the holographic direction, can be seen as the renormalization parameter [59]. This actually means the renormalization group flow is geometrized in the bulk. In a certain sense, therefore, the black hole can be seen as a highly renormalized infrared (IR) version of our microscopic, ultraviolet (UV) boundary theory. A critical system is said to have a diverging correlation length ξ, which signals scale invariance. We can also introduce a correlation time t related as $\xi = t^{-1/z}$, thus, z, the dynamical critical exponent, represents the relative scaling of time and space [26]. Normally, we would expect $z = 1$, or some finite number, however, in AdS/CFT, our systems acquire a critical timescale while still having a finite correlation length. This is called semi-locality [32] and is a GR effect: light signals coming from a point on the boundary will reach only a finite patch of the horizon - light coming from different points may or may not overlap depending on the boundary distance. Effectively, it means that $z \to \infty$ in these systems. Exactly this type of anomalous scaling behaviour has been found in cuprates [42]. Using normal renormalization intuition, we can see a UV entity like the lattice imposed on the CFT gets renormalized towards the IR black hole horizon: however, if it becomes relevant, irrelevant or marginal actually depends on the length scale of the lattice (the lattice spacing). We will go into more detail in the Results section 3.8.

The AdS/CFT correspondence allows us to perform calculations on a wide range of strongly correlated, critical systems. A case in point is the quark-gluon plasma: the deconfined state of matter ruled by the strong force, a soup of quarks and gluons at extremely high temperatures, as, for example, the universe perhaps was directly after the Big Bang. The viscosity is found to obey [35]:

$$\frac{\eta}{s} \approx \frac{\hbar}{4\pi k_B} \tag{30}$$

where s is the entropy density and η is the shear viscosity. It is conjectured that this is a lower bound for strongly correlated systems in general, and therefore called the minimal viscosity. It has been found that the quark-gluon plasma in a particle collider setting indeed satisfies this bound [38].

Version of January 13, 2021– Created January 21, 2022 - 14:18

A central result of the theory of Quantum criticality (like our CFT) is that it predicts a universal momentum relaxation time $\tau_\hbar$:

$$\tau_\hbar = \frac{\hbar}{k_B T} \tag{31}$$

This is conjectured to be the shortest possible timescale permissible by nature in which equilibrium can be reached, therefore called Planckian dissipation [57]. By dimensional analysis, it can be shown that the Minimal viscosity is an incarnation of Planckian dissipation [58]. Furthermore, when fed into the Drude formula for conductivity (5), it predicts linear in T resistivity at all T, protected by a very strong principle (namely, strongly correlated quantum critical matter must satisfy this relaxation time bound). Perhaps most importantly, it actually rolls out of DC transport data for both hole and electron doped cuprates [37]. Finally, this is independent of material properties - as has observed in a wide range of strongly correlated electron systems [31]. The bottom line is that relaxation times of the form (31) are the hallmark of quantum criticality, meaning many-body physics, and harder to explain from single quasiparticle behaviour [28].

1.10 Hydrodynamics

Let us return to the phase diagram in figure 1: what do we expect to lie between a perfect solid (Mott insulator) and a perfect gas (Fermi liquid)? Of course, we should expect a regime of hydrodynamics. This seems to be a sidetrack at first: weren't we interested in densely entangled, quantum critical behaviour as described by black holes? How would hydrodynamics factor in? It has been shown, however, that the full Navier-Stokes equations can be obtained in the boundary of AdS/CFT by studying the dynamical near-horizon geometry in the bulk - therefore, there exists a Fluid/Gravity duality in the AdS/CFT correspondence [11]. Furthermore, hydrodynamics describes the flow of conserved quantities under a system that is brought out of equilibrium, over distances and timescales which are long compared to the local relaxation times - and with strange metals and quantum critical, holographic metals, we know we are dealing with the shortest relaxation timescale achievable (equation (31)) and so these conditions are actually easily achieved. Thus, we expect these systems to behave very hydrodynamically, meaning with minimal viscosities, nearing perfect fluids, as local equilibrium is reached super quick. (Hydrodynamics in electron systems is rare: in normal metals, collision times are short compared to relaxation times, preventing local equilibrium from be-

Version of January 13, 2021– Created January 21, 2022 - 14:18

ing reached. It may be observable in graphene, as that is clean enough for electron motion to collectivize, since scattering is rare.)

Another key insight is that Drude theory is applicable as long as momentum relaxes slowly - and is not inherently related to the scattering particle picture Drude himself envisioned. If we interpret τ as the particle lifetime, which makes sense at least in a Fermi liquid situation, quasiparticle excitations are the shortest possible, and we in essence have a highly unparticle-like type of matter, effectively described by hydrodynamics. Finally, it has been verified that strange metals shows a Drude peak in AC resistivity [40]. This concludes our tour of the history of the theory of transport in metals, which has brought us back to the start: Drude theory.

To analyze our data in full generality, we need some adjustments to the plain vanilla Drude sketched in section 1.2. First, we need to recognize that when we introduce a lattice, we are in fact not only breaking spatial symmetry, but also break rotational symmetry (the Lie group SO(2) gets replaced by the finite point group specific to the crystal lattice we choose). Thus, not only linear momentum relaxes: angular (transverse) momentum will leak out of our system as well and we have a second relaxation time τ_T in addition to τ_L. In ordinary metals these times will be identical, however, the Hall angle conundrum in strange metals gives reason to believe these may be different and have different temperature dependence. Therefore, our EoM become:

$$\frac{dP_{x,L}}{dt} = eE_x - \frac{1}{\tau_L}P_{x,L} \tag{32}$$

$$\frac{dP_{x,T}}{dt} = \omega_C P_y - \frac{1}{\tau_T}P_{x,T} \tag{33}$$

and likewise for P_Y. Here, $\omega_c = qEB/m$ is the cyclotron frequency. Proceeding as in section 1.2 we now obtain two components of our DC conductivity matrix as in [20]:

$$\sigma_{xx} = \frac{\omega_p \tau_L}{1 + (\omega_c \tau_T)^2} \tag{34}$$

$$\sigma_{xy} = \sigma_{xx}\omega_c \tau_T \tag{35}$$

A further adjustment we need to make concerns the expressions for the plasmon and cyclotron frequencies, as they should now be in terms of our relativistic theory of hydrodynamics, instead of colliding particles. They are obtained by taking $m \to (\epsilon + P)$ (the mass becomes the energy density and pressure) and $q \to n$ (the single particle charge become the charge density). Below are given the full expression for electric, thermal and

thermo-electric resistivities as found in [15]:

$$\begin{aligned} \sigma^{-1} &= \frac{1}{n^2}\hat{R} \\ \alpha^{-1} &= \frac{1}{ns}\hat{R} \\ \bar{\kappa}^{-1} &= \frac{1}{sT^2}\hat{R} \end{aligned} \tag{36}$$

where s is the entropy density and $\hat{R}$ is a 2×2 matrix defined as:

$$\hat{R} = (\epsilon + P) \begin{pmatrix} \frac{1}{\tau_L} & -\omega_c \frac{\tau_T}{\tau_L} \\ \omega_c \frac{\tau_T}{\tau_L} & \frac{1}{\tau_L} \end{pmatrix} \tag{37}$$

The DC transport coefficients can be efficiently calculated by evaluating hydrodynamical response very close to black hole horizon [6]. This amounts to solving the Navier-Stokes equations using the hairy AdS black hole as a background over which our electrodynamically charged liquid flows (as water would flow over pebbles, the riverbed here being a dyonic, hairy black hole).

One further comment that needs to be made is that equations (36) are not full expressions for the DC resistivities in full generality in a holographic context. While it is true a hydrodynamical mode governs DC transport - termed the coherent sector, as it is generated by the coherent motion of conserved quantities - there is also incoherent transport in all quantum critical systems, as our boundary CFT is an example of. Incoherent transport is generated by the collective diffusion of energy and charge in such a system [24]. This incoherent conductivity σ_Q is additive:

$$\sigma_{\text{Full}} = \sigma_{\text{Drude}} + \sigma_Q \tag{38}$$

Its contribution is expected to be small at the low temperatures we are interested in. We will go into more detail regarding Drude versus incoherent transport in the Results section 3.1.

1.11 Weak Lattice Hydrodynamics

Forgetting the holographic origin of our fluid for a moment, we can wonder what transport coefficients are predicted for a charged fluid flowing through a lattice in presence of a magnetic field purely by relativistic hydrodynamics. In the small lattice strength (A) limit, exact results can be

Version of January 13, 2021– Created January 21, 2022 - 14:18

obtained [4]. For the resistivity, we have:

$$\rho = \frac{\epsilon + P}{n^2} \begin{pmatrix} (\frac{1}{\tau_0} + \frac{1}{\tau_S}) & -(\omega_c + \frac{1}{\tau_A}) \\ (\omega_c + \frac{1}{\tau_A}) & (\frac{1}{\tau_0} + \frac{1}{\tau_S}) \end{pmatrix} \tag{39}$$

Note that the thermodynamical quantities comprising the Drude weight are here taken at their homogeneous ($A = 0$) values, as opposed to equation (36) where they are defined in-lattice. We immediately see weak lattice hydrodynamics in a magnetic field predicts two extra relaxation rates, τ_S and τ_A (symmetric and anti-symmetric), proportional to both the magnetic field strength and the lattice strength. More precisely, hydrodynamics predicts scaling as: $\frac{1}{\tau_0} \sim A^2$, $\frac{1}{\tau_S} \sim A^2B^2$ and $\frac{1}{\tau_S} \sim A^2B$ in the small A regime. Having these analytical results provides a useful check for transport coefficients as calculated holographically in the near horizon geometry, as they must coincide with above findings for small A. Furthermore, it shows we expect a magnetic field dependent term in the longitudinal relaxation rate for such a hydrodynamic system, τ_S. Namely, there exists a direct transformation between equation (36) and (39): $\frac{1}{\tau_0} = \frac{1}{\tau_0} + \frac{1}{\tau_S}$ and $\frac{\omega_c \tau_T}{\tau_l} = \omega_c + \frac{1}{\tau_A}$. This immediately shows that there is a B^2 term present in τ_L in the weak lattice case. Lastly, we know:

$$\frac{\omega_c \tau_A}{1 + \omega_c \tau_A} = \frac{\Gamma_T}{\Gamma_L} > 1 \tag{40}$$

(where $\Gamma \equiv \frac{1}{\tau}$) since the relaxation rate in the transverse direction must always exceed that in the longitudinal direction. For this to hold, $\tau_A < 0$, and is therefore perhaps better thought of as a shift of cyclotron frequency than a relaxation rate per se. These relaxation times with proper scaling are indeed found in Results section 3.7, and the range of validity is checked.

2 Method

2.1 Linear Differential Equations

Any differential equation may be written in the form:

$$\mathcal{F}[y] = 0. \tag{41}$$

We are given $\mathcal{F}$, which are the equations of motion (EoM) of our system in addition to any boundary conditions on y, and are then tasked with finding the solution y. y may be the position and momentum of a single

particle as function of t, or of many particles. It may also be a field or many different fields defined on every point in space, as is the case in our AdS/CFT setup.

We can take all non-derivative containing terms of $\mathcal{F}$ to the RHS and write:

$$\mathcal{G}[y] = b. \tag{42}$$

When $\mathcal{G}$ is a linear operator, we are dealing with a linear differential equation and we have:

$$\mathcal{G}[\lambda y_1 + \mu y_2] = \lambda \mathcal{G}[y_1] + \mu \mathcal{G}[y_2]. \tag{43}$$

In this case, solving the differential equation is conceptually very simple and amounts to calculating the inverse $\mathcal{G}^{-1}$ so that:

$$y = \mathcal{G}^{-1}[b]. \tag{44}$$

When solving differential equations numerically, you are limited by a physical computer with finite RAM, which is why you have to work with finite differences. Again, conceptually very simply, this amounts to interpreting all differential operators $\frac{d}{dx}$ as matrices, which give the differences between neighbouring points in fields or in time and proceeding as usual. Instead of calculating the inverse matrix directly, other methods exist like LU-decomposition [12] - but they all amount to solving equation (44).

2.2 Non-Linear Differential Equations

When our differential operator $\mathcal{F}$ is no longer linear, it cannot be written as a matrix and efficiently inverted numerically. A ploy is to hazard a guess y_0' which gives us:

$$\mathcal{F}[y_0'] = r \tag{45}$$

where $r \neq 0$ if our guess is wrong. Suppose our guess is almost right, however, and we can expand around the solution as $y_0' = y + \delta y$:

$$\mathcal{F}[y + \delta y] = \mathcal{F}[y] + \frac{d}{dy}\mathcal{F}[y]\delta y + O(\delta y^2) = r \tag{46}$$

If our guess was right enough, we can ignore higher order terms, and since y was the solution we have:

$$\frac{d}{dy}\mathcal{F}[y]\delta y = r \tag{47}$$

Version of January 13, 2021– Created January 21, 2022 - 14:18

This is again a linear equation, which we can solve with the method from the previous section. We can update our guess as $y_1' = y_0' - \delta y$ and then repeat this procedure until $|r| <$ threshold. This gives us an efficient method of approaching a solution to a non-linear differential equation if we have a good ansatz to start with. (We are ignoring derivatives of δy, however, these can be taken into account by calculating the Jacobian of $\mathcal{F}$ and proceeding as above.)

2.3 Implementation

In our study of a RN holographic metal, we wish to solve Einstein's equations and Maxwell's equations in an AdS space. Notoriously non-linear, this is only exacerbated by the fact that we wish to implement a lattice on the boundary. Thus, computations where performed on the ALICE supercomputing cluster in Leiden, using the PETSc C-library differential equation solvers [3].

The Einstein-Maxwell action is given by:

$$S_{\text{EM}} = \int dx^4 \sqrt{-g} \left(R - 2\Lambda - F^{\mu\nu} F_{\mu\nu} \right) \tag{48}$$

where g is the metric determinant, R the Ricci scalar and Λ the cosmological constant (which gives us the inherent curvature of AdS space). We take AdS_3 to describe a two dimensional boundary metal. We obtain the EoM:

$$R_{\mu\nu} - \Lambda g_{\mu\nu} = \frac{1}{2} \left(F_{\mu\nu} F^{\rho}_{\nu} - \frac{1}{4} g_{\mu\nu} F_{\rho\sigma} F^{\rho\sigma} \right) \tag{49}$$

$$\nabla_{\mu} F^{\mu\nu} = 0 \tag{50}$$

The chemical potential on the boundary is modulated as a boundary condition to implement the lattice:

$$\mu(x, y) = \bar{\mu} \left(1 + \sin(Gx) \sin(Gy) \right). \tag{51}$$

For a more detailed derivation and how the field components are related to solid state observables and thermodynamics, see [5].

In short, we were able to acquire numerical solutions to above equations - RN metals - for a given temperature T, lattice strength A, magnetic field strength B and lattice vector G (inverse of lattice spacing). For the non-linear solver, the ansatz was a simple homogeneous $A = 0$ AdS RN black hole at arbitrary values of the other parameters. A could then be slowly increased, and taking sufficiently small steps guaranteed convergence of the algorithm even to low temperatures ($T \approx 10^{-4}\mu$). Such a

Version of January 13, 2021– Created January 21, 2022 - 14:18

background can then be used to perform Navier-Stokes computations on the black hole horizon to give DC (electric, thermal and thermo-electric) transport properties. Furthermore, the energy, pressure and charge density can be calculated from the fields approaching the boundary - the entropy is acquired from the black hole via the Bekenstein formula (29). All thermodynamic quantities are given in units of chemical potential μ, and B is given in units of μ^2. All backgrounds were calculated on a grid size of $40 \times 40 \times 50$ where 50 is the holographically radial direction.

2.4 Numerical Accuracy

Apart from bugs in the code and structural errors, when doing numerical work you are dealing with finite numerical accuracy. Akin to an experimental setting, we had to make sure our numerical noise-to-signal ratio was sufficiently small. We tested for numerical accuracy in multiple ways: firstly, simply checking the differential solver indicated it properly converged. Another straightforward method is rerunning code and comparing outcomes. Yet another method was varying grid sizes, which should not have a significant effect on outcomes. A last method was checking basic identities, for example: $\sigma_{xx} = \sigma_{yy}$ and $\sigma_{xy} = -\sigma_{yx}$. These were found not to hold in presence of significant numerical noise (no convergence). Notably, the gamma ratio peak in section 3.6, which is perhaps most suspect, is not affected by varying grid sizes. Only results which held up to the above tests are reported.

3 Results

3.1 Drude Fit

We wish to study the coherent Drude transport of the holographic RN metal - to do that we must first know if transport is indeed governed by Drude forms. As mentioned in section 1.10, we expect an incoherent mode of transport σ_Q to also be present in a critical system. The set of equations is underdetermined: we fit six independent transport coefficients (σ_{xx}, σ_{xy}, α_{xx}, α_{xy}, κ_{xx}, κ_{xy}) with two relaxation times, Γ_L and Γ_T. To examine the accuracy of the Drude fit, we extract the relaxation rates from σ and reconstruct the thermal and thermo-electric conductivities using equations (36). The plasmo and cyclotron frequency were determined thermodynamically. The deviation from the actual numerical transport coefficients is an indication of the accuracy of the Drude model. In figure 2 we see that

Version of January 13, 2021– Created January 21, 2022 - 14:18

over a range of temperature and lattice strength, the model holds well for low temperatures and lattice strengths. Deviations all fall withing 10% within the domain we are interested in. For higher temperatures, on the order of μ, σ_Q starts to dominate. Similar deviations are seen when varying B and G, with the highest fields and lattice vectors giving the largest deviations, and all within 10%.

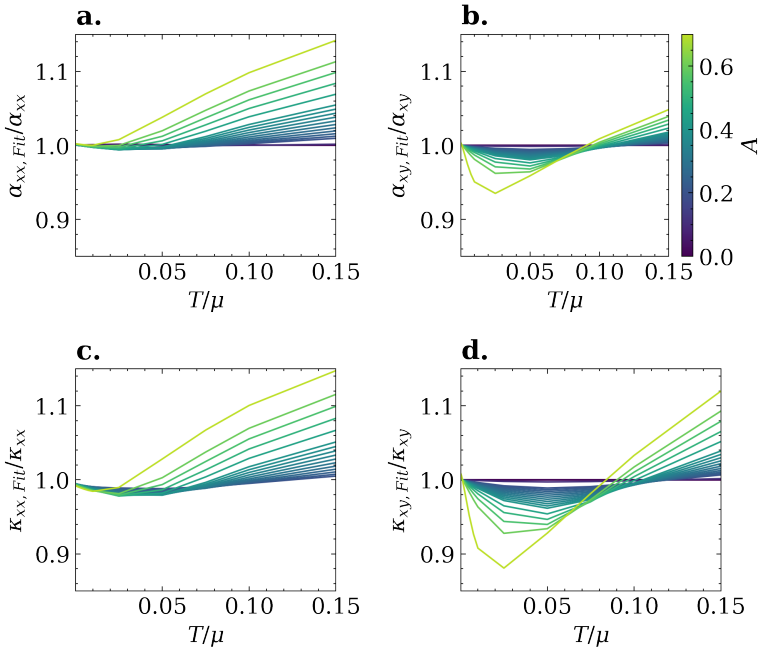

Figure 2: **a.** *Deviation of the thermo-electrical conductivity from that predicted by the Drude model, with relaxation rates extracted from σ at $B = 0.001\mu^2$ and $G = 0.1\mu$. For $T > 0.1\mu$ we have an error of the order of 10^{-1} at the strongest lattices.* **b.** *Same as a for the transverse component. Here the deviation follows a sinusoidal-like distribution with amplitudes set by lattice strength, however, errors stay withing 5%.* **c.** *Same as a for the thermal conductivity.* **d.** *Same as b for the transverse thermal conductivity.*

3.2 Magnetic Insulator

In figure 3a we see σ_{xx} *increase* with temperature at low A and low T/μ - the characteristic behaviour of an insulator - while our holographic material shows ordinary metallic temperature dependence in the rest of phase space. Perhaps puzzling at first, this is actually normal Drude behaviour for a two dimensional metal with a vanishingly small relaxation rate in the

Version of January 13, 2021– Created January 21, 2022 - 14:18

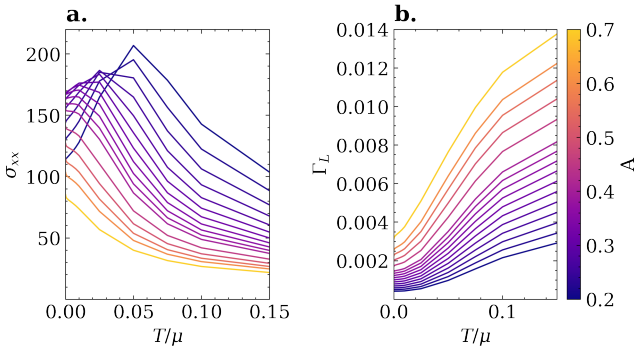

Figure 3: **a.** *The longitudinal conductivity in presence of a magnetic field of strength $B = 0.001\mu^2$ and Umklapp vector $G = 0.1\mu$ at at range of temperature and lattice strength. Note that for $A < 0.3$ and $T/\mu < 0.05$, the conductivity displays insulator like temperature dependence.* **b.** *The longitudinal relaxation rate Γ_L from a Drude fit of a. It displays normal behaviour at all values of A and T, increasing with temperature.*

presence of a magnetic field. We have:

$$\sigma_{xx} = \frac{\omega_p^2 \tau}{1 + (\omega_c \tau)^2}. \tag{52}$$

As $A \to 0$, the relaxation time, of course, diverges: $\tau \to \infty$. We get that $(\omega_c \tau)^2 \gg 1$ and so

$$\sigma_{xx} \approx \frac{\omega_p^2 \tau}{(\omega_c \tau)^2} \sim \frac{1}{\tau}. \tag{53}$$

Now, if τ decreases with temperature, which causes metallic temperature dependence in the conductivity normally, in this limit, it actually causes the conductivity to *increase*. In figure 3b we indeed see that this is the case. Thus, it is an interplay between the two dimensionality, the presence of a magnetic field and the zero lattice limit which causes the singular behaviour. The order of limits is important: were we to take $B \to 0$ first, then $\omega_c \to 0$, and we would get the normal DC Drude expression (5), which would still give metallic conductivity in the $\tau \to \infty$ limit. From here, we will mostly ignore this regime, as the case where momentum relaxes on timescales of millennia is not quite relevant to the study of non-Fermi liquids and does not imply a breakdown of the applicability of Drude theory.

Version of January 13, 2021– Created January 21, 2022 - 14:18

3.3 Wiedemann Franz Law & Nernst Effect

As derived in section 1.2, in normal metals at low temperatures (and very high temperatures), the ratio $\kappa_{xx}/(\sigma_{xx}T) \equiv L$ is temperature independent, as heat and charge are both transported by the same carriers (electrons). In hydrodynamical systems and quantum critical systems especially, momentum and current relax via very different kinematics, and they are expected to be violate the Wiedemann-Franz law as derived by Hartnoll et al. [21]. Furthermore, they expect $\kappa_{xx}/(\sigma_{xx}T) \sim 1/T^2$. As seen in figure 4a, we do see strong deviations from temperature independence, however, we do not find $1/T^2$ behaviour.

As explained in section 1.1, the Nernst effect concerns the thermoelectric transport. The Nernst signal is defined as $\theta_{yx} = -(\rho\alpha)_{yx}$ and is expected to be positive for hydrodynamical vortex systems, while negative for positive for quasiparticle systems [45]. As we see in figure 4b, we indeed find a positive Nernst signal. Furthermore, it was derived by Hartnoll et al. for the Nernst signal to be linear in field B for a strongly correlated quantum critical fluid [27]. We also find this to be the case for the RN metal. Finally, the Nernst coefficient, $\nu = \theta_{yx}/B$ is predicted to scale as $1/T^4$ in the same paper. However, we find the Nernst coefficient to *increase* with temperature, as seen in figure 4c.

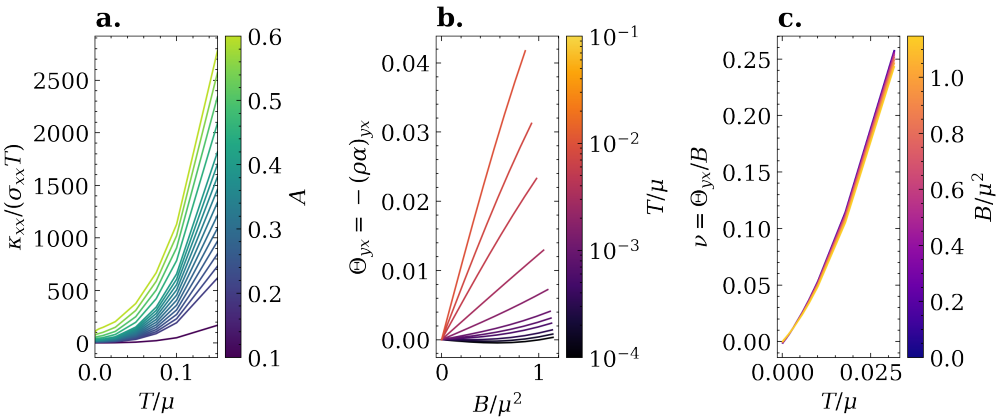

Figure 4: **a.** *The ratio of thermal and electrical conductivity over a range of temperatures at different lattice strengths for $G = 0.1\mu$. As it is not a constant, the RN metal violates the Wiedemann-Franz law.* **b.** *The Nernst signal as a function of the field B at different temperatures at $A = 0.5$ and $G = 0.1\mu$. Except at very low temperatures, it is found to follow linear in field behaviour.* **c.** *The Nernst coefficient over a range of temperature for different field strengths - the same data as in b - found to increase with temperature. As expected, it is almost totally field independent.*

Version of January 13, 2021– Created January 21, 2022 - 14:18

3.4 Holographic Umklapp: Hartnoll-Hoffman Scaling

Momentum relaxes out of our electron system via the Umklapp process. In section 1.4 this was shown to lead to $\Gamma \sim T^2$ temperature dependence in a Fermi liquid. It has been shown that in locally critical systems ($z \to \infty$) this temperature dependence instead follows $\Gamma_L \sim T^{\alpha_L}$, where $\alpha_L(G)$ is a function of the lattice momentum/Umklapp vector. Hartnoll and Hofman find in [25] (equation (28) and (35)):

$$\alpha_L = \sqrt{5 + 4k^2 - 4\sqrt{1 + 2k^2}} - 1 \tag{54}$$

Note that due to differences in conventions we have: $k = \frac{3}{2\sqrt{2}}G$. In figure 5a we see that Γ_L displays neat power law in T behaviour for $G/\mu \geq 0.4$. We can extract the T exponents and in figure 5b we see that these exponents indeed match the predicted Hartnoll-Hofman scaling at both high and low lattice strength. Finally, at high lattice strength, one can turn on a magnetic field and extract the transverse temperature exponent $\Gamma_T \sim T^{\alpha_T}$. In figure 5 we see that these do not differ significantly over our chosen range of Umklapp vectors.

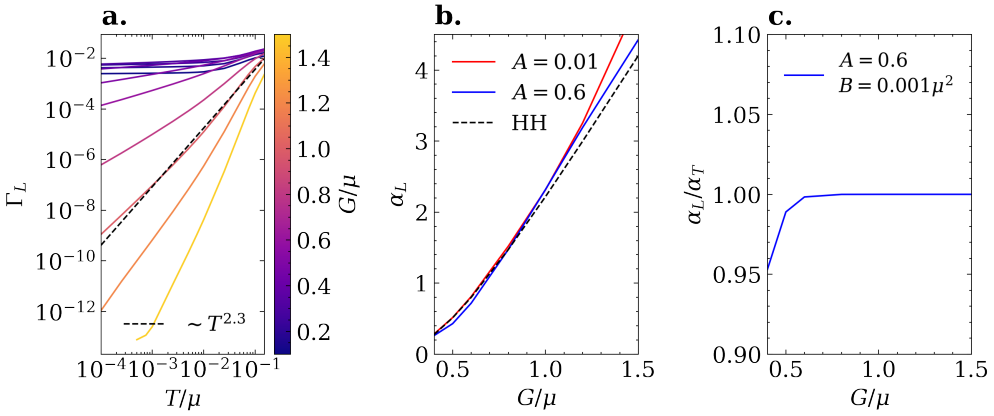

Figure 5: **a.** *Longitudinal relaxation rate on a log-log plot versus temperature at different lattice momenta at $A = 0.6$ and no magnetic field. There is clear power law behaviour in T for $G/\mu \geq 0.4$, while below that value, the lines acquire a kink at $T/\mu \approx 10^{-2}$. The dashed line shows the power law fit for $G/\mu = 1$.* **b.** *Temperature exponents of $Gamma_L$ as a function of lattice momentum for $A = 0.01$ and $A = 0.6$. The dashed line represents equation 54.* **c.** *The ratio of longitudinal and transverse relaxation rate temperature exponents versus lattice momentum at $A = 0.6$ and $B/\mu^2 = 0.001$.*

Version of January 13, 2021– Created January 21, 2022 - 14:18

3.5 The First Law of Thermodynamics

In a hydrodynamic system, we assume the time scales and length scales to be long as compared to local relaxation times, and can therefore assume local equilibrium to hold in the fluid. Concretely, this means the laws of thermodynamics hold at a local scale. Here, we will focus on the first law in integrated form, essentially giving an expression for the internal energy of a fluid element:

$$\epsilon + P = TS + \mu\rho \tag{55}$$

We calculate these values by averaging over the AdS boundary (so in actuality, $\mu\rho \equiv \overline{\mu\rho}|_{\partial_{\text{AdS}}}$) to obtain the thermodynamical expressions of our holographic metal. All thermodynamic values are implicitly averaged from now on. An exception is the entropy, which is calculated by determining the area of the BH horizon in the centre of AdS via the Bekenstein formula (29) by integrating over the metric.

In the homogeneous case, with $A = 0$ and $B = 0$, the solution is equal to the analytical solution of a Reissner Nordström black hole, and equation (55) is satisfied trivially at all temperatures - providing an easy and basic check for the holographic code.

Next, we stay in the homogeneous case, but turn on a magnetic field. We expect an extra magnetization term to enter expression (55):

$$\epsilon + P = TS + \mu\rho + MB \tag{56}$$

where $M = \mu B$ is the magnetization. As we see in figure 6a, this identity is satisfied in our system.

However, things get hairier when we start modulating the chemical potential on the boundary. As we see in figure 6b, when plotting the expression $\epsilon + P - \mu\rho - TS - MB$, which should be identically zero, this is only satisfied in the $A = 0$ case. Some term must be ill-defined, and a likely candidate is the entropy S, as it is not clear that the Bekenstein expression should also hold for a corrugated black. Moreover, we are dealing with a fluid, and thus we have a local entropy density at every point in space (the entropy of the fluid element which can be thought of as a large N system which is, in itself, in equilibrium) - it is not straightforward how to go from these local entropy densities to the total system entropy. Although these things may all be true, they actually cannot solve the current issue, as we see that in the $T \to 0$ limit in figure 6b, the identity is actually also not satisfied for larger A, where we can ignore the TS term. For a further discussion, see section 5.2.

Finally, as we see in figure 6c, the characteristic zero temperature entropy of the RN black hole is retrieved by our system. When the two hori-

Version of January 13, 2021– Created January 21, 2022 - 14:18

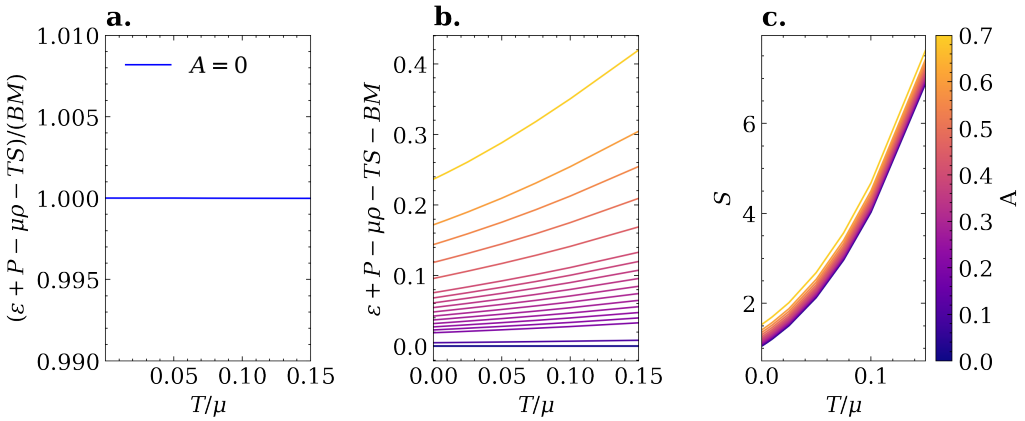

Figure 6: **a.** *In the homogeneous case with a magnetic field B, the following equation must be satisfied: $\epsilon + P - \mu\rho - TS = MB$ where M is the magnetization. We see that this is perfectly satisfied at all temperatures. Shown here is $B = 0.001\mu^2$, however, this holds for any B.* **b.** *Here we have plotted the expression of the first law such that it should be identically zero, in presence of a field $B = 0.001\mu^2$ and $G = 0.1\mu$. We see that this is only satisfied in the homogeneous $A = 0$ case. Therefore, we can conclude that in the presence of a lattice, the terms are adjusted in some non-trivial way. See section 5.2 for a further discussion.* **c.** *As the temperature goes to zero, there is a residual entropy left at all lattice strengths. Zero temperature entropy is characteristic of a Reissner-Nordström black hole - for a discussion of the implications, see section 5.1.*

zons of the RN black hole coincide, we end up with an extremal black hole with finite radius but zero temperature [14]. For a discussion of the implications for transport in the boundary CFT, see section 5.1.

3.6 The Gamma Ratio Peak

A key experiment in strange metals is the 'Hall effect conundrum': while longitudinal resistivity goes as $\rho_{xx} \sim T$, the Hall Angle scales quadratically $\Theta_H \sim T^2$. It is proposed an anisotropic Drude model as in section 1.10 can explain this phenomenon via two different relaxation rates, Γ_L and Γ_T, with different temperature dependencies, as $\rho_{xx} \sim \Gamma_L$ and $\Theta_H = \rho_{yx}/\rho_{xx} \sim \Gamma_T$ [20]. Here we investigate the temperature dependence of the Gamma ratio Γ_T/Γ_L of our holographic Reissner-Nordström metal. In figure 7c we see that, in the isotropic limit where A is small or T is high, the Gamma ratio is temperature independent, however, in the low temperature strong lattice regime, we break isotropy and the Gamma ratio acquires a temperature dependence.

Version of January 13, 2021– Created January 21, 2022 - 14:18

Although nothing like $\sim T$ as seen in strange metals, this does provide a proof of principle that in Holography, longitudinal and transverse relaxation rates need not scale identically. As to why the ratio displays a peak of increasing height with increasing lattice strength, we are still in the dark, although it is clear the 'peak-like' behaviour stems from Γ_T as seen in figure 7b. Furthermore, as seen in equation (36), all Hall resistivities go as $\rho_{xy} \sim \frac{\Gamma_T}{\Gamma_L}$ with some proportionality constant set purely by thermodynamical quantities. On the one hand, this means the Gamma ratio peak is directly visible in the observable Hall resistivity as in 7d. On the other hand, it implies that in the isotropic case, where $\Gamma_L = \Gamma_T$, Hall resistivities are set entirely by thermodynamical quantities, namely: $\rho_{xy} = -\frac{\omega_c}{\omega_p^2}$ and likewise for thermal and electro-thermal Hall resistivities. This is displayed in figure 7d, where the transport coefficient and thermodynamical ratio coincide in the small A regime. It was further found the Gamma peak is suppressed as one increases the magnetic field, as shown in figure 11a in the Appendix.

3.7 Weak Lattice Hydro

In section 1.11 the transport of a relativistic fluid in presence of weak spatial symmetry breaking and a magnetic field was expressed in terms of three relaxation rates. Here we investigate the weak lattice limit and explore where this regime breaks down. In terms of the resistivity, the relaxation rates are:

$$\frac{1}{\tau_0} = \omega_p^2 \rho_{xx}(B=0) \sim A^2 \tag{57}$$

$$\frac{1}{\tau_S} = \omega_p^2 \rho_{xx} - \frac{1}{\tau_0} = \omega_p^2 (\rho_{xx}(B) - \rho_{xx}(B=0)) \sim A^2 B^2 \tag{58}$$

$$\frac{1}{\tau_A} = \omega_p^2 \rho_{yx} - \omega_C \sim A^2 B \tag{59}$$

Note that the thermodynamic quantities are here as defined in the homogeneous ($A = B = 0$) limit, $\tau_A < 0$ and that τ_S sets the magneto-resistance. We see in figure 8a that predicted scaling in A is found for all three, and starts to deviate from $A > 0.1$, which is the upper bound of the weak lattice limit. At this bound, we find the predicted B for τ_S and τ_A holds up to magnetic fields strengths of $B \approx 0.001\mu^2$. For reasonable magnetic fields ($B < 0.001\mu^2$) we see that $1/\tau_S$ and $1/\tau_A$ are only slight corrections to $1/\tau_0$ and ω_C, as expected.

Version of January 13, 2021– Created January 21, 2022 - 14:18

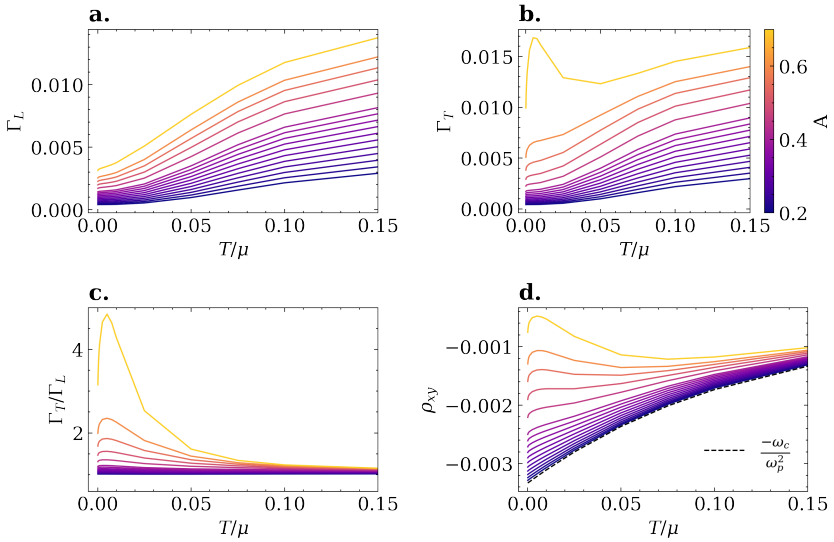

Figure 7: **a. & b.** *The longitudinal and transverse relaxation rates as function of temperature of a range of lattice strengths at $B = 0.001\mu^2$ and $G = 0.1\mu$. We see that for $A = 0.7$, the peak becomes pronounced in Γ_T, although it is also present at lower strengths.* **c.** *The gamma ratio at $B = 0.001\mu^2$ and $G = 0.1\mu$. For small A, the system becomes isotropic and $\Gamma_T/\Gamma_L = 1$. At higher A, the ratio has clear temperature dependence, and thus the relaxation rates scale differently in T.* **d.** *The hall resistivity as function of temperature over the same range of A, at identical B and G. The gamma ratio peak is directly visible. In the isotropic limit, the Hall resistivity becomes determined entirely by thermodynamics: the dashed line which is $-\omega_c/\omega_p^2$ at $A = 0.2$ coincides with the data.*

3.8 Renormalization of the Lattice

As touched upon in section 1.9, values on the AdS boundary get renormalized towards the black hole horizon. Strictly speaking, the lattice is irrelevant towards the horizon - why can we then speak of DC transport in presence of a lattice when this is calculated on the horizon?

The answer lies in the fact that we are dealing with *geometrized* renormalization: the intrinsic curvature of AdS sets a length scale over which renormalization takes place, and areas further away than this distance are causally disconnected and do not renormalize. As explained in [32], the boundary effectively splits into many domains, each which independently acts like a conformal liquid. Are we able to see this effect in our RN metal? By varying G/μ we vary the lattice spacing. When G is small, the spacing is large, and when the period of the lattice is larger than the AdS length scale, it cannot effectively renormalize because of the GR implications, and

Version of January 13, 2021– Created January 21, 2022 - 14:18

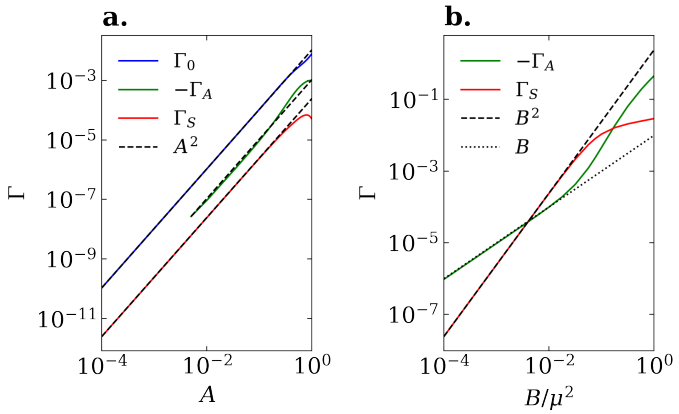

Figure 8: *All data is at $G = 0.1\mu$.* **a.** *Log-log plot of all three relaxation rates as a function of A at $B = 0.001\mu^2$. For very small values of A, the off-diagonal elements of ρ become numerically unstable, which is why Γ_A can only be accurately shown for $A > 0.01$. Deviation from A^2 behaviour starts at $A = 0.1$.* **b.** *Log-log plot of Γ_S at $A = 0.1$ as function of B; B^2 behaviour is seen in up to $B \approx 0.05\mu^2$.* **c.** *Log-log plot of $-\Gamma_A$ at $A = 0.1$ as a function of B; linear in B behaviour holds up to $B \approx 0.01\mu^2$.*

the lattice survives in the boundary. Oppositely, when G is big, many lattice periods fit into one conformal domain, and these will be evened out and become irrelevant on the horizon. Exactly this behaviour is what we see in figure 9a & b. Furthermore, the relaxation rates also diminish when $G \to 0$: this is simply the lattice spacing becoming so huge, that the lattice becomes very sparse and does not impede the movement of the fluid ($G \to 0$ is equal to the lattice spacing going to infinite, in which we recover our spatially homogeneous system with no lattice). It is these two competing effects which produce the Γ peak as a function of G. Lastly, in figure 9c we see the Gamma ratio saturating at 1 a lot earlier than the rates themselves going to zero: this indicates that the system becomes effectively isotropic at $G > 0.4\mu$, while becoming very anisotropic at lower G. Temperature seems to have little effect on the ratio as a function of G.

Note that $\Gamma_T/\Gamma_L \geq 1$ as each rotation can effectively be decomposed in two translations: the relaxation of angular momentum must be at least as big as that of longitudinal momentum.

3.9 Magneto Resistance

When we turn on a magnetic field perpendicular to our plane of conductivity, electrons will start to perform cyclotron motion which hinders

Version of January 13, 2021– Created January 21, 2022 - 14:18

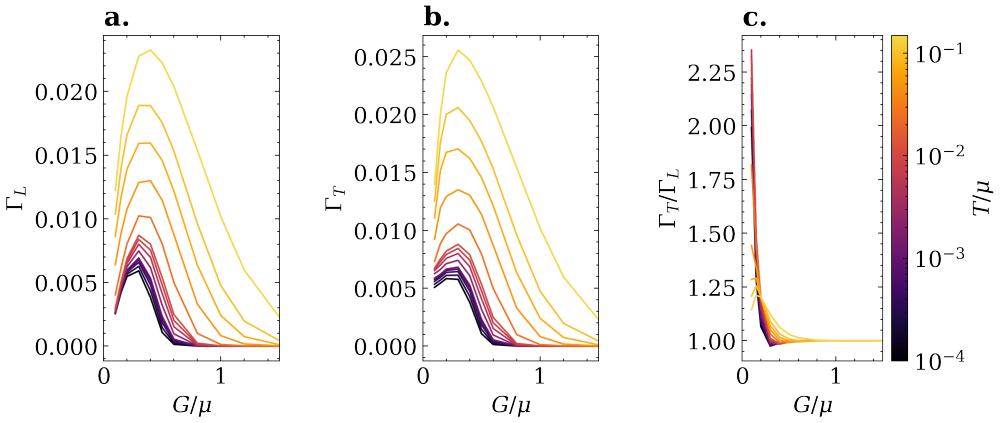

Figure 9: **a.** *Longitudinal relaxation rate as a function of the lattice vector G over a range of different temperatures at a strong lattice $A = 0.5$ and $B = 0.001\mu^2$. We see that the rate fizzles out to zero as we take G larger due to renormalization effects kicking in. For small G, the spacing grows so big that it becomes unnoticeable for transport. The rate increases with temperature as expected.* **b.** *The same as for a except for transverse relaxation. We see less of a diminishing for small G.* **c.** *The ratio of relaxation rates as a function of G. Note that it saturates to 1 for $G > 0.5\mu$ as the system become isotropic and that this happens for smaller G than the reduction of the rates themselves.*

them from crossing straight through: the result is an increase in resistance, magneto-resistance(MR). It is defined as the percentage of resistance caused by the magnetic field in terms of the zero field resistance:

$$\mathrm{MR} = \frac{\Delta\rho}{\rho(B=0)} = \frac{\rho(B) - \rho_0}{\rho_0} \tag{60}$$

In standard isotropic, quasiparticle Drude theory, this is captured by supposing two types of charge carriers (electrons and holes) with opposite charge, such that $\vec{J} = \vec{J_1} + \vec{J_2} = (\sigma_1 + \sigma_2)\vec{E}$. One can go through the typical Drude procedure in this case to obtain an expression for ρ_{xx} which gives:

$$\mathrm{MR}_{\mathrm{quasi}} \sim (\omega_C \tau)^2. \tag{61}$$

As ω_c, we expect $MR \sim B^2$. However, as we have seen, Drude theory applies to any system which relaxes momentum slowly, and so also to a hydrodynamical substance. A notable difference, however, is that in a fluid, we cannot have *different* charge carriers flowing independently without interacting as in the ideal Fermi gas/liquid theory: one cannot pump water and oil through a pipe in opposite directions. Thus we are dealing with

Version of January 13, 2021– Created January 21, 2022 - 14:18

a single charge carrying substance. As we have seen in section 1.10, this gives a resistivity:

$$\rho_{xx} = \frac{\Gamma_L}{\omega_p^2} \tag{62}$$

Where would magneto resistance originate from in this case when we no longer have a cyclotron frequency factor left? This is normally interpreted as that single carrier Drude does not predict MR. However, in our RN metal, we do measure MR. Thus, it must be the relaxation rate Γ itself which internalizes the magnetic field - as opposed to the two particle Drude case, where Γ was B independent. As we see in figure 10a, we also measure a B^2 MR in our RN metal for reasonable field strengths. Therefore, suppose we write: $\Gamma_L = \Gamma_0(1 + \Gamma_B B^2)$. Then we have:

$$\mathrm{MR}_{\mathrm{hydro}} \sim \Gamma_B B^2 \tag{63}$$

A clear difference between the two-quasiparticle picture and the hydrodynamical picture is that the MR goes as the relaxation *time* in the former, and the relaxation *rate* in the latter. Suppose that relaxation rates always increase with temperature, then an immediate consequence would be that the derivatives of the MR in the quasiparticle and hydro cases would differ by sign: $\frac{d\mathrm{MR}_{\mathrm{quasi}}}{dT} < 0$ but $\frac{d\mathrm{MR}_{\mathrm{hydro}}}{dT} > 0$. However, things do not appear to be that simple, as when we inspect the temperature behaviour of Γ_B in our system, we find that it increases drastically with temperature, see figure 10b. Thus, it may not be as easy as to interpret Γ_B as simply a relaxation rate.

Note that in the weak lattice hydrodynamical language of section 1.11, such a magnetic field dependent component of the longitudinal relaxation rate was predicted in the form of $\frac{1}{\tau_S} \sim B^2$. Such field dependent relaxation rates may therefore be a hall-mark of hydrodynamics coupled to electrodynamics.

4 Conclusion

While far from being a one-to-one model for strange metals, the local quantum critical, dual to RN holographic metal does seem a promising lead for investigating some of the peculiar aspects of strange metal transport. Most notably, it displays an angular momentum relaxation temperature dependence which is different from the longitudinal, as shown in section 3.6, which could eventually explain the anomalous temperature scaling of the Hall angle in strange metals. Furthermore, it was found thermo-

Version of January 13, 2021– Created January 21, 2022 - 14:18

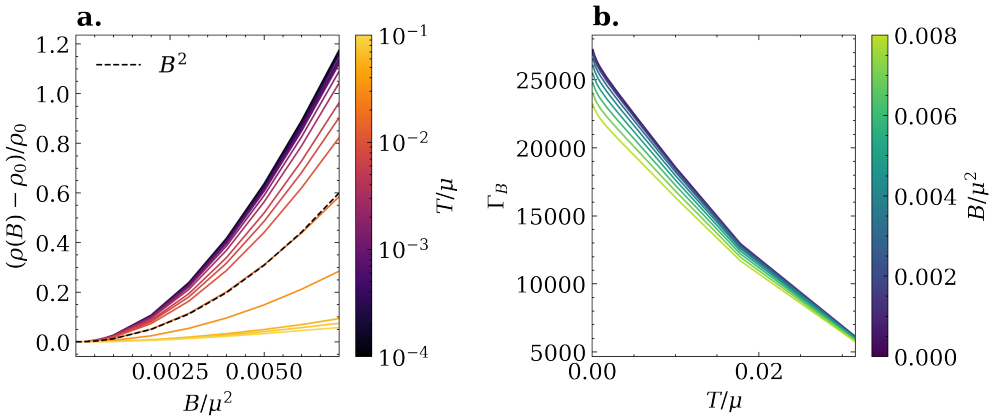

Figure 10: **a.** *Magneto-resistance as a function of field strength at differing temperatures for $A = 0.5$ and $G = 0.1\mu$. The MR follows B^2 behaviour as indicated by the dashed line. Note that the MR* decreases *with temperature.* **b.** *The relaxation rate which couples to the magnetic field component in the longitudinal relaxation rate. It is almost B independent, which means that Γ_L has a field component which is almost perfectly quadratic (perhaps related to numerical noise at low temperatures). Also, it decreases with temperature, which is perhaps surprising for a relaxation rate.*

electric transport in the RN metal can be accurately described by Drude theory at low temperatures in section 3.1. The RN metal was found to violate the Wiedemann-Franz law and show a Nernst signal characterizing vortex motion 3.3. It was found the relaxation rate follows a temperature power law as predicted from Holographic Umklapp at larger Umklapp vectors in section 3.4. In the case of a highly corrugated black hole, it was found the expression for the energy undergoes some non-trivial adjustment which has not yet been properly understood, and is not linked to the entropy, as described in section 3.5. In the weak lattice limit, the RN metal transport was found to behave in good agreement with theory of hydrodynamics with a perturbatively small lattice and magnetic field, as seen in section 3.7. It was found that the effects of semi-locality of AdS/CFT are visible in the renormalization of the lattice as expected in section 3.8. Finally, it was shown in section 3.9 that in a hydrodynamical metal system, the magnetoresistance is set by the relaxation rate Γ acquiring a field dependent term, as opposed to the MR entering via the cyclotron frequency, also in correspondence with the weak lattice prediction.

Version of January 13, 2021– Created January 21, 2022 - 14:18

5 Discussion

5.1 Choice of Black Hole

The RN black hole is characterized by its singular zero temperature entropy [14]. This is a surprisingly deep problem for the study of transport in a holographic metal, as we are dealing with hydrodynamical flow. In a fluid, momentum relaxes via the shear drag: momentum in the x direction diffuses into the y direction by internal friction, and if the fluid experiences a resistance along the boundary of the flow (for example, a pipe), this causes the fluid as a whole to slow down and lose momentum. Therefore, there is a relationship between the momentum relaxation rate and the viscosity, known as Poiseuille's law:

$$\Gamma = \frac{\eta}{(\epsilon + P)l^2} \tag{64}$$

where l is the relevant length scale of the system (pipe radius, for example). Now, if we plug in our expression for the minimal viscosity (equation (30)), which is known to be an incarnation of Planckian dissipation, which is known to characterize quantum critical systems, we get the following simple relation:

$$\Gamma \sim S. \tag{65}$$

Therefore, if our BH entropy does not go to zero linearly as the temperature does, we do not expect a linear to zero behaviour of the relaxation rate, as is seen in strange metals.

A way around this is to introduce a scalar dilaton field in addition to the Einstein-Maxwell action (48). The dyonic black hole was studied by Gubser and Rocha in this setting and was found to obtain a entropy proportional to temperature at low temperature [23]. Therefore, in a holographic metal dual to a Gubser-Rocha black hole, we can expect to see the linear in T resistivity at low temperatures.

5.2 First Law of Thermodynamics

As we saw in section 3.5 of the results, the first law is not satisfied at zero temperature. Therefore, one might conclude there is a problem with either ϵ, P, μ or ρ. However, since the Drude model fits all transport data (see section 3.1), something must be going right. On closer inspection we see that the $\epsilon + P$ term drops out when comparing different transport coefficients. This indicates that the error is most likely to lie in these terms. Fur-

Version of January 13, 2021– Created January 21, 2022 - 14:18

thermore, the pressure P is defined as the diagonal element of the Stress-Energy tensor in the boundary $T_{xx} = T_{yy}$ (in a square lattice). In the case of broken spatial symmetries (the lattice), these terms no longer correspond to conserved charges associated with spatial translational symmetry - one may wonder what the pressure that features in the first law is. In short: what is the relation between thermodynamics and conserved Noether currents in broken symmetries? More thought is probably required to solve this issue.

Furthermore, all this has ignored the TS term so far: it is not excluded, and perhaps even unlikely, that there may be an issue with the entropy - after all, does the Bekenstein entropy expression (29) hold in the case of a highly corrugated black hole? Hair, of course, increases the area to a significant amount. Are we supposed to integrate the area along the horizon, or are we supposed to calculate the average Schwarzschild radius and go from there? These questions still need answering before a in depth analysis of the thermodynamics of our Holographic metal can be performed.

6 Appendix

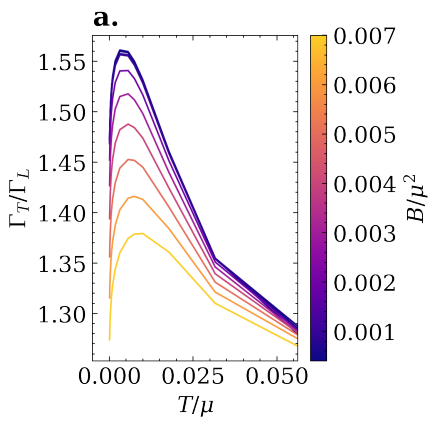

Figure 11: **a.** *The Gamma ratio as a function of T for a range of field strengths at $A = 0.5$ and $G = 0.1\mu$. The peak is subdued by increasing the field strength.*

Version of January 13, 2021– Created January 21, 2022 - 14:18

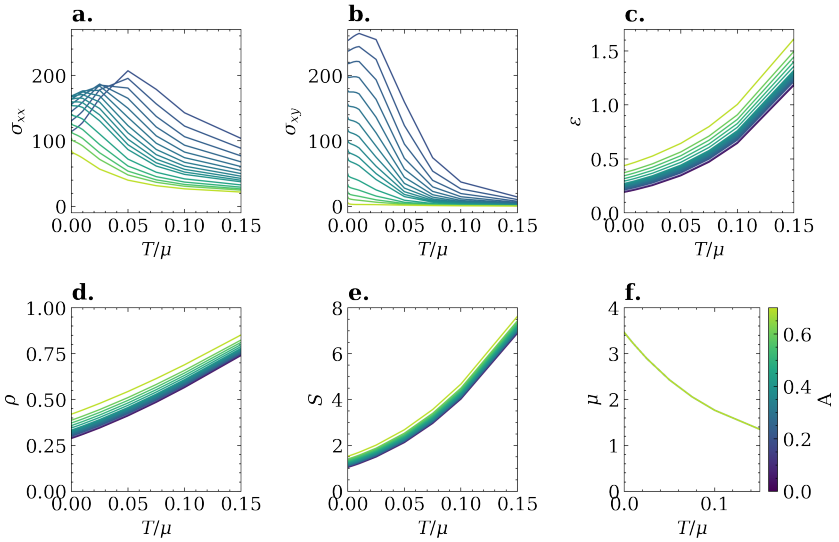

Figure 12: *Conductivities and thermodynamical variables as a function of temperature for a range of lattice strengths at $B = 0.001\mu^2$ and $G = 0.1\mu$. Note that $\epsilon = 2P$ is always found to hold, and P is therefore omitted. Also note that μ is not in units of μ but in units of horizon radius, so that it is not identically 1.*

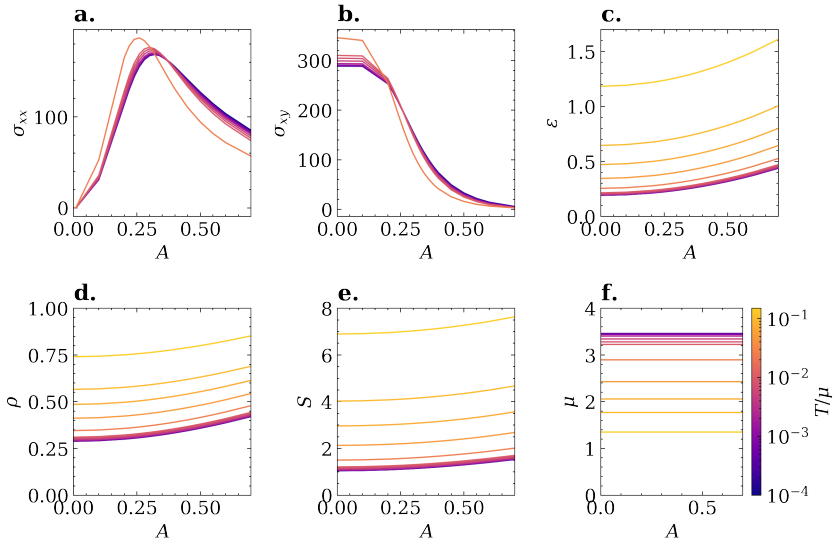

Figure 13: *Conductivities and thermodynamical variables as a function of lattice strength for a range of temperatures at $B = 0.001\mu^2$ and $G = 0.1\mu$. Note that ϵ, ρ and S are all of the form: $\propto A^2 + \text{const.}$, where constant means not a function of A.*

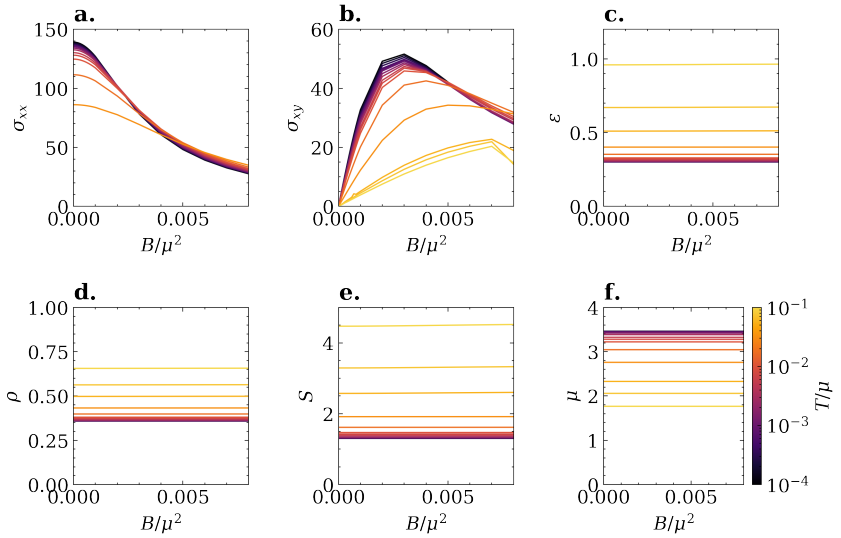

Figure 14: *Conductivities and thermodynamical variables as a function of magnetic field strength for a range of temperatures at $A = 0.5$ and $G = 0.1\mu$.*

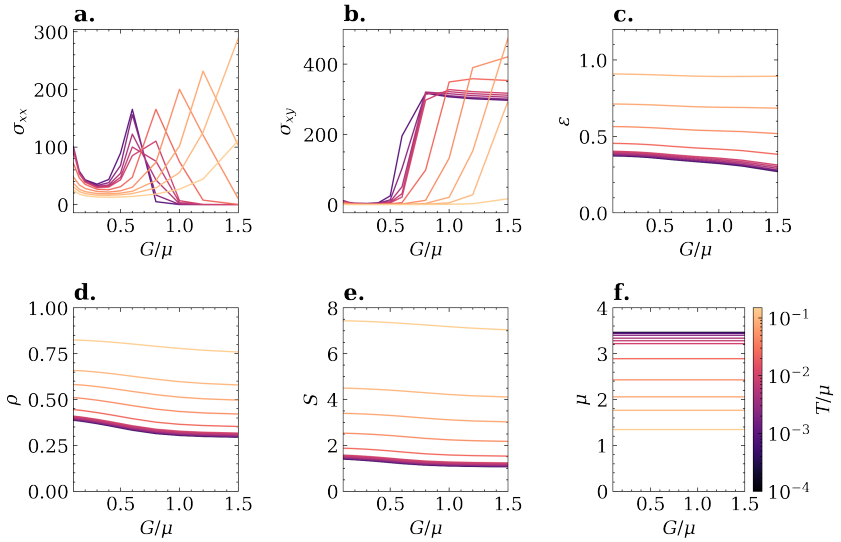

Figure 15: *Conductivities and thermodynamical variables as a function of the lattice vector for a range of temperatures at $A = 0.6$ and $B = 0.001\mu^2$. The peak in conductivities as a function of G is elaborated on in section 3.8.*

Bibliography

[1] P. W. Anderson. Plasmons, gauge invariance, and mass. *Phys. Rev.*, 130:439–442, Apr 1963.

[2] J. Ayres, M. Berben, M. Äulo, Y.-T. Hsu, E. van Heumen, Y. Huang, J. Zaanen, T. Kondo, T. Takeuchi, J. R. Cooper, and et al. Incoherent transport across the strange-metal regime of overdoped cuprates. *Nature*, 595(7869):661â666, Jul 2021.

[3] Satish Balay, Shrirang Abhyankar, Mark F. Adams, Steven Benson, Jed Brown, Peter Brune, Kris Buschelman, Emil M. Constantinescu, Lisandro Dalcin, Alp Dener, Victor Eijkhout, William D. Gropp, Václav Hapla, Tobin Isaac, Pierre Jolivet, Dmitry Karpeev, Dinesh Kaushik, Matthew G. Knepley, Fande Kong, Scott Kruger, Dave A. May, Lois Curfman McInnes, Richard Tran Mills, Lawrence Mitchell, Todd Munson, Jose E. Roman, Karl Rupp, Patrick Sanan, Jason Sarich, Barry F. Smith, Stefano Zampini, Hong Zhang, Hong Zhang, and Junchao Zhang. PETSc Web page. `https://petsc.org/`, 2021.

[4] F.A. Balm, S. Arend, M.A. Janse, D. Rodriguez Fernandez, A. Krikun, K.E. Schalm, and J. Zaanen. Magneto-transport of the reissner-nordstrom holographic metal in a periodic potential. *In Preparation*, 2022.

[5] Floris Balm, Alexander Krikun, Aurelio Romero-BermÃºdez, Koenraad Schalm, and Jan Zaanen. Isolated zeros destroy fermi surface in holographic models with a lattice. *Journal of High Energy Physics*, 2020(1), Jan 2020.

[6] Elliot Banks, Aristomenis Donos, and Jerome P. Gauntlett. Thermoelectric dc conductivities and stokes flows on black hole horizons, 2015.

[7] J. Bardeen, L. N. Cooper, and J. R. Schrieffer. Theory of Superconductivity. *Physical Review*, 108(5):1175–1204, December 1957.

[8] Bertram Batlogg and Chandra M Varma. The underdoped phase of cuprate superconductors. *Physics World*, 13(2):33–38, feb 2000.

[9] J. G. Bednorz and K. A. Muller. Possible high Tc superconductivity in the Ba-La-Cu-O system. *Z. Phys. B*, 64:189–193, 1986.

[10] Jacob D. Bekenstein. Universal upper bound on the entropy-to-energy ratio for bounded systems. , 23(2):287–298, January 1981.

[11] Sayantani Bhattacharyya, Shiraz Minwalla, Veronika E Hubeny, and Mukund Rangamani. Nonlinear fluid dynamics from gravity. *Journal of High Energy Physics*, 2008(02):045â045, Feb 2008.

[12] James R. Bunch and John E. Hopcroft. Triangular factorization and inversion by fast matrix multiplication. *Mathematics of Computation*, 28(125):231–236, 1974.

[13] Marco M Caldarelli, Ãscar J.C Dias, and Dietmar Klemm. Dyonic ads black holes from magnetohydrodynamics. *Journal of High Energy Physics*, 2009(03):025â025, Mar 2009.

[14] Sean Carroll. *Spacetime and Geometry: An Introduction to General Relativity*. Benjamin Cummings, 2003.

[15] Richard A. Davison and Blaise GoutÃ©raux. Dissecting holographic conductivities. *Journal of High Energy Physics*, 2015(9), Sep 2015.

[16] Jules de Launay. The isotope effect in superconductivity. *Phys. Rev.*, 93:661–665, Feb 1954.

[17] P. Drude. Zur Elektronentheorie der Metalle. *Annalen der Physik*, 306(3):566–613, January 1900.

[18] Freeman J. Dyson and A. Lenard. Stability of Matter. I. *Journal of Mathematical Physics*, 8(3):423–434, March 1967.

[19] S. Coda et al. Overview of the tcv tokamak program: scientific progress and facility upgrades. *Nuclear Fusion*, 57(10):102011, 2017.

[20] Xuanbo Feng, Maarten Berben, Silvia Cassanelli, Linda Neubrand, Leonard de Jager, Yingkai Huang, Nigel Hussey, Jan Zaanen, and Erik van Heumen. Disentangling the transport properties in the 2201 cuprates with optical spectroscopy. *In Preparation*, 2022.

[21] R. Franz and G. Wiedemann. Ueber die wÃ€rme-leitungsfÃ€higkeit der metalle, January 1853.

[22] David J. Griffiths. *Introduction to Quantum Mechanics (2nd Edition)*. Pearson Prentice Hall, 2nd edition, April 2004.

[23] Steven S. Gubser and Fabio D. Rocha. Peculiar properties of a charged dilatonic black hole inads5. *Physical Review D*, 81(4), Feb 2010.

[24] Sean A. Hartnoll. Theory of universal incoherent metallic transport. *Nature Physics*, 11(1):54â61, Dec 2014.

[25] Sean A. Hartnoll and Diego M. Hofman. Locally critical resistivities from umklapp scattering. *Physical Review Letters*, 108(24), Jun 2012.

[26] Sean A. Hartnoll and Andreas Karch. Scaling theory of the cuprate strange metals. *Physical Review B*, 91(15), Apr 2015.

[27] Sean A. Hartnoll, Pavel K. Kovtun, Markus MÃŒller, and Subir Sachdev. Theory of the nernst effect near quantum phase transitions in condensed matter and in dyonic black holes. *Physical Review B*, 76(14), Oct 2007.

[28] Sean A. Hartnoll and Andrew P. Mackenzie. Planckian dissipation in metals, 2021.

[29] S. W. Hawking. Black hole explosions? , 248(5443):30–31, March 1974.

[30] J. Hubbard. Electron correlations in narrow energy bands. *Proceedings of the Royal Society of London. Series A, Mathematical and Physical Sciences*, 276(1365):238–257, 1963.

[31] N. E. Hussey â, K. Takenaka, and H. Takagi. Universality of the mottâioffeâregel limit in metals. *Philosophical Magazine*, 84(27):2847â2864, Sep 2004.

[32] Nabil Iqbal, Hong Liu, and MÃ¡rk Mezei. Semi-local quantum liquids. *Journal of High Energy Physics*, 2012(4), Apr 2012.

[33] H. Kamerlingh Onnes. Further experiments with liquid helium. C. On the change of electric resistance of pure metals at very low temperatures etc. IV. The resistance of pure mercury at helium temperatures. *Koninklijke Nederlandse Akademie van Wetenschappen Proceedings Series B Physical Sciences*, 13:1274–1276, January 1910.

[34] B. Keimer, S. A. Kivelson, M. R. Norman, S. Uchida, and J. Zaanen. High temperature superconductivity in the cuprates, 2014.

[35] P. K. Kovtun, D. T. Son, and A. O. Starinets. Viscosity in strongly interacting quantum field theories from black hole physics. *Phys. Rev. Lett.*, 94:111601, Mar 2005.

[36] L. D. Landau. The Theory of a Fermi Liquid. *Zh. Eksp. Teor. Fiz.*, 30(6):1058, 1956.

[37] A. Legros, S. Benhabib, W. Tabis, F. LalibertÃ©, M. Dion, M. Lizaire, B. Vignolle, D. Vignolles, H. Raffy, Z. Z. Li, and et al. Universal t-linear resistivity and planckian dissipation in overdoped cuprates. *Nature Physics*, 15(2):142â147, Nov 2018.

[38] Matthew Luzum and Paul Romatschke. Conformal relativistic viscous hydrodynamics: Applications to rhic results at $\sqrt{s_{NN}} = 200$ gev. *Phys. Rev. C*, 78:034915, Sep 2008.

[39] Juan Maldacena. *International Journal of Theoretical Physics*, 38(4):1113â1133, 1999.

[40] D. van der Marel, H. J. A. Molegraaf, J. Zaanen, Z. Nussinov, F. Carbone, A. Damascelli, H. Eisaki, M. Greven, P. H. Kes, and M. Li. Quantum critical behaviour in a high-tc superconductor. *Nature*, 425(6955):271â274, Sep 2003.

[41] W. L. McMillan. Transition temperature of strong-coupled superconductors. *Phys. Rev.*, 167:331–344, Mar 1968.

[42] M. Mitrano, A. A. Husain, S. Vig, A. Kogar, M. S. Rak, S. I. Rubeck, J. Schmalian, B. Uchoa, J. Schneeloch, R. Zhong, G. D. Gu, and P. Abbamonte. Anomalous density fluctuations in a strange metal. *Proceedings of the National Academy of Sciences*, 115(21):5392–5396, 2018.

[43] C. Montonen and D. Olive. Magnetic monopoles as gauge particles? *Physics Letters B*, 72(1):117–120, December 1977.

[44] N. F. Mott and R. Peierls. Discussion of the paper by de Boer and Verwey. *Proceedings of the Physical Society*, 49(4S):72–73, August 1937.

[45] V. Oganesyan and Iddo Ussishkin. Nernst effect, quasiparticles, and d-density waves in cuprates. *Physical Review B*, 70(5), Aug 2004.

[46] N. P. Ong, T. W. Jing, T. R. Chien, D. A. Brawner, Z. Z. Wang, and J. M. Tarascon. The hall effect and magnetoresistance of the high-temperature cuprate superconductors. In Yasuhiro Iye and Hiroshi Yasuoka, editors, *The Physics and Chemistry of Oxide Superconductors*, pages 247–254, Berlin, Heidelberg, 1992. Springer Berlin Heidelberg.

[47] Lars Onsager. Reciprocal relations in irreversible processes. i. *Phys. Rev.*, 37:405–426, Feb 1931.

[48] R Perin. The superconducting magnet system for the LHC. page 9 p, Nov 1990.

[49] Shinsei Ryu and Tadashi Takayanagi. Aspects of holographic entanglement entropy. *Journal of High Energy Physics*, 2006(08):045â045, Aug 2006.

[50] Subir Sachdev. Where is the quantum critical point in the cuprate superconductors? *physica status solidi (b)*, 247(3):537â543, Feb 2010.

[51] Subir Sachdev. *Quantum Phase Transitions*. Cambridge University Press, 2 edition, 2011.

[52] Andreas Schilling, Marco Cantoni, J. Guo, and H. Ott. Superconductivity above 130 k in the hg-ba-ca-cu-o system. *Nature*, 363:56–58, 05 1993.

[53] T. J. Seebeck. Ueber die magnetische Polarisation der Metalle und Erze durch Temperaturdifferenz, January 1826.

[54] Gerard 't Hooft. Dimensional reduction in quantum gravity. *arXiv: General Relativity and Quantum Cosmology*, 1993.

[55] Baptiste Vignolle, A. Carrington, R Cooper, M. French, A. Mackenzie, Cyril Jaudet, D. Vignolles, Cyril Proust, and N. Hussey. Quantum oscillations in an overdoped high-tc superconductor. *Nature*, 455:952–5, 11 2008.

[56] Dieter Vollhardt. *Pair Correlations in Superfluid Helium 3*, pages 205–220. Springer US, Boston, MA, 1998.

[57] J. Zaanen. Superconductivity - why the temperature is high. *Nature*, 430:512–3, 08 2004.

[58] Jan Zaanen. Lectures on quantum supreme matter, 2021.

[59] Jan Zaanen, Yan Liu, Ya-Wen Sun, and Koenraad Schalm. *Holographic Duality in Condensed Matter Physics*. Cambridge University Press, 2015.